Lanthanide Luminescence for Biomedical Analyses and Imaging

Jean-Claude G. Bünzli*

Laboratory of Lanthanide Supramolecular Chemistry, École Polytechnique Fédérale de Lausanne (EPFL), BCH 1402, CH-1015 Lausanne, Switzerland, and Department of Advanced Materials Chemistry, WCU Center for Next Generation Photovoltaic Systems, Korea University, Sejong Campus, 208 Seochang, Jochiwon, Chung Nam 339-700, Republic of Korea

Received November 5, 2009

Contents

Jean-Claude Bünzli is an active researcher in the field of co-ordination, supramolecular, and biological chemistry of the lanthanide ions. He earned a degree in chemical engineering in 1968 and a Ph.D. in 1971 from the École Polytechnique Fédérale de Lausanne (EPFL). He spent two years at the University of British Columbia (Canada) and one year at the Swiss Federal Institute of Technology in Zürich before being appointed at the University of Lausanne in 1974 and at EPFL in 2001 as a full professor of inorganic chemistry. Since September 2009, he also holds a WCU professorship at Korea University, Sejong Campus, Jochiwon, South Korea. His research focuses on the design and/or self-assembly of building blocks for photoluminescent materials and lanthanide luminescent bioprobes, with particular emphasis on the imaging of cancerous cells and tissues.

1. Introduction

Gaining greater understanding of the structural and functional properties of living systems is a key challenge in biology and medicine. On a more practical side, the diagnosis and treatment of cancer is requiring individualized approaches[1] which, in turn, necessitates better and faster pathological analyses as well as highly contrasted, real-time bioimages. Noninvasive methodologies are required in order to perturb the investigated systems and organs as little as possible, and optical emissive probes are emerging as strong candidates for this purpose. Indeed, when appropriate wavelengths are used, penetration depth may be substantial and light can reach regions of complex molecular edifices which are not accessible to other molecular probes.[2] In addition, the emitted photons are easily detected by highly sensitive devices and techniques, including single-photon detection. When the lifetime of the excited emitting level is long enough, time-resolved detection (TRD) considerably enhances the signal-to-noise ratio. Organic luminophores are commonly fluorescent and therefore highly emissive because the transition is parity allowed, but they are subject to photobleaching and TRD necessitates sophisticated methodologies in view of the very large emission rates: 10^7-10^9 s^{-1}, corresponding to excited state lifetimes between 100 and 1 ns. Semiconductor quantum dots (CdSe nanocrystals with 2−10 nm diameter) and their bioconjugates are potential substitutes, being highly luminescent, tunable in the entire visible range, and displaying a superior photostability compared to organic luminophores. They have been used for both in vitro analyses and in vivo imaging, but their introduction into biology and medicine is slow because they

* To whom correspondence should be addressed. E-mail: jean-claude.bunzli@epfl.ch.

10.1021/cr900362e
Published on Web 02/12/2010

suffer from flaws which are tricky to remedy such as the difficulty in getting near-infrared (NIR) emission for deeper tissue penetration, the high toxicity of cadmium and selenium, and their short circulation half-time preventing long-term imaging or cell-tracking studies.[3] Trivalent lanthanide ions, Ln^{III}, present another alternative to organic luminescent stains in view of their singular properties, enabling easy spectral and time discrimination of their emission bands which span both the visible and NIR ranges.

The first staining of biological cells with lanthanides dates back to 1969 when bacterial smears (*Escherichia coli* cell walls) were treated with aqueous ethanolic solutions of europium thenoyltrifluoroacetonate, henceforth appearing as bright red spots under mercury lamp illumination,[4] but further experiments had to wait a long time. In fact, attention on luminescent lanthanide bioprobes started in the mid-1970s when Finnish researchers in Turku proposed Eu^{III}, Sm^{III}, Tb^{III}, and Dy^{III} polyaminocarboxylates and β-diketonates as luminescent sensors in time-resolved luminescent (TRL) immunoassays.[5,6] This new technology generated a broad interest and subsequent developments such as homogeneous TRL assays,[7] optimization of bioconjugation methods for lanthanide luminescent chelates,[8] and time-resolved luminescence microscopy (TRLM)[9] resulted in applications of lanthanide luminescent bioprobes (LLBs)[10,11] in many fields of biology, biotechnology, and medicine, including analyte sensing[12] and tissue[13,14] and cell imaging[15,16] as well as monitoring drug delivery.[17]

This review addresses the problematic of lanthanide luminescent bioprobes from the standpoint of their photophysical and biochemical properties; a broad overview of the various applications in which LLBs have been applied is given. No attempt is made to provide comprehensive coverage of the extensive literature pertaining to this field; instead, illustrative examples are described and the reader is referred to the numerous well-focused review articles which appeared during the past five years.

2. Lanthanide Luminescence

2.1. Basic Facts

The intricate optical properties of the trivalent lanthanide ions, hereafter Ln^{III}, are fascinating and originate in the special features of the electronic $[Xe]4f^n$ configurations ($n = 0-14$). These configurations generate a rich variety of electronic levels, the number of which is given by $[14!/n!(14 - n)!]$, translating into 3003 for Eu^{III} and Tb^{III}, for instance.[18] They are characterized by three quantum numbers, S, L, and J, within the frame of Russel−Saunders spin−orbit coupling scheme. The energies of these levels are well-defined due to the shielding of the 4f orbitals by the filled $5s^25p^6$ subshells, and they are a little sensitive to the chemical environments in which the lanthanide ions are inserted. As a corollary, inner-shell 4f−4f transitions which span both the visible and near-infrared (NIR) ranges are sharp and easily recognizable (Figure 1, Table 1). In addition, because these transitions are formally parity forbidden, the lifetimes of the excited states are long, which allows the use of time-resolved detection, a definitive asset for bioassays,[19,20] and luminescence microscopy.[9]

The only drawback of f−f transitions, their faint oscillator strengths, may in fact be turned into advantages. Indeed, Weissman demonstrated in 1942 that excitation of lanthanide complexes into the ligand states results in metal-centered

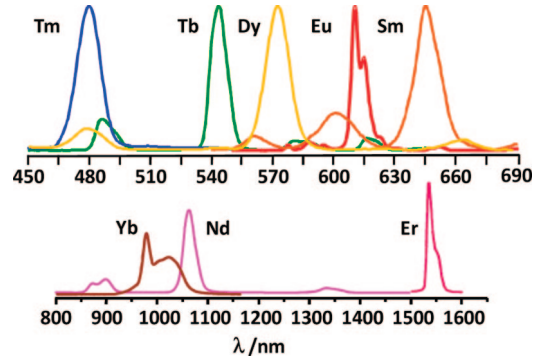

Figure 1. Luminescence spectra of some lanthanide tris(β-diketonates). (Redrawn from ref 21. Copyright Wiley.)

luminescence.[22] Part of the energy absorbed by the organic receptor(s) is transferred onto Ln^{III} excited states, and sharp emission bands originating from the metal ion are detected after rapid internal conversion to the emitting level. The phenomenon is termed sensitization of the metal-centered luminescence (also referred to as antenna effect) and is quite complex. Several energy migration paths may be involved, e.g., exchange or superexchange (Dexter), dipole−dipole, or dipole−multipole (Förster) mechanisms,[23] which entail the participation of several ligand levels, singlet, triplet, and/or intraligand charge transfer (ILCT) states. A commonly observed energy migration path though goes through the long-lived triplet state(s) of the ligand(s).[24] Alternatively, other states may funnel energy onto the metal ion such as intracomplex ligand-to-metal (LMCT) charge transfer states,[25] 4f5d states,[26] or metal-to-ligand (^{1}MLCT, ^{3}MLCT) charge transfer states from chromophores containing d-transition metal ions[27] such as Cr^{III},[28] Re^{I},[29] Ru^{II},[30,31] Os^{II},[32,33] Co^{III},[34] Ir^{III},[35] or Pt^{II}.[36−38] These d-ions are essentially used for the sensitization of NIR luminescence.[39] The sensitization process generates two advantages. First, while Ln^{III} ions display a negligible Stokes' shift upon direct excitation, owing to the inner nature of the 4f-orbitals, ligand excitation results in pseudo Stokes' shifts which are often far larger than those of organic fluorophores, henceforth allowing easy spectral discrimination of the emitted light. Second, Ln^{III} ions are usually good quenchers of triplet states so that photobleaching is substantially reduced.

Lanthanide ions are involved in three types of transitions, LMCT, 4f−5d, and intraconfigurational 4f−4f.[40] The former two usually occur at energies too high to be relevant for bioapplications, so that only the latter are discussed here. We note, however, that low-lying LMCT states may have detrimental effect on the emissive properties of easily reducible Ln^{III} ions (e.g., Eu^{III}, Sm^{III}, or Yb^{III}). Some ions are fluorescent ($\Delta S = 0$), some are phosphorescent ($\Delta S > 0$), and some are both. Similarly to absorption, emission of light is due to two main types of transitions, the parity allowed magnetic dipole transitions (MD, selection rules: $\Delta L = 0$, $\Delta J = 0, \pm 1$ but $J = 0$ to $J' = 0$ forbidden), and the parity forbidden electric dipole transitions (ED; ΔL, $\Delta J \leq 6$; 2, 4, 6, if J or $J' = 0$; $J = 0$ to $J' = 0$ forbidden). When the Ln^{III} ion is inserted into a chemical environment, noncentrosymmetric interactions allow the mixing of electronic states of opposite parity into the 4f wave functions and ED transitions become partly allowed; they are termed induced (or forced) ED transitions. The intensity of some of these transitions is particularly sensitive to the nature of the metal-ion environment, and these transitions are called

Table 1. Selected Luminescent Properties of Ln^{III} Ions[a]

Ln	G	I	F	λ/μm or nm[b]	gap/cm^{-1}[b]	τ^{rad}/ms[b]
Ce	$^2F_{5/2}$	5d	$^2F_{5/2}$	tunable, 300−450		
Pr	$^3H_4$	$^1D_2$	$^3F_4$, $^1G_4$, $^3H_4$, $^3H_5$	1.0, 1.44, 600, 690	6940	(0.05[c]−0.35)
		$^3P_0$	^3H_J (J = 4−6)	490, 545, 615	3910	(0.003[c]−0.02)
		$^3P_0$	^3F_J (J = 2−4)	640, 700, 725		
Nd	$^4I_{9/2}$	$^4F_{3/2}$	^4I_J (J = 9/2−13/2)	900, 1.06, 1.35	5400	0.42 (0.2−0.5)
Sm	$^6H_{5/2}$	$^4G_{5/2}$	^6H_J (J = 5/2−13/2)	560, 595, 640, 700, 775	7400	6.26
		$^4G_{5/2}$	^6F_J (J = 1/2−9/2)	870, 887, 926, 1.01, 1.15		
		$^4G_{5/2}$	$^6H_{13/2}$	877		
Eu[d]	$^7F_0$	$^5D_0$	^7F_J (J = 0−6)	580, 590, 615, 650, 720, 750, 820	12300	9.7 (1−11)
Gd	$^8S_{7/2}$	$^6P_{7/2}$	$^8S_{7/2}$	315	32100	10.9
Tb	$^7F_6$	$^5D_4$	^7F_J (J = 6−0)	490, 540, 580, 620	14800	9.0 (1−9)
				650, 660, 675		
Dy	$^6H_{15/2}$	$^4F_{9/2}$	^6H_J (J = 15/2−9/2)	475, 570, 660, 750	7850	1.85 (0.15−1.9)
		$^4F_{15/2}$	^6H_J (J = 15/2−9/2)	455, 540, 615, 695	1000	3.22[b]
Ho	$^5I_8$	$^5S_2$	^5I_J (J = 8,7)	545, 750	3000	0.37 (0.51[c])
		$^5F_5$	$^5I_8$	650	2200	0.8[c]
		$^5F_5$	$^5I_7$	965		
Er[e]	$^4I_{15/2}$	$^4S_{3/2}$	^4I_J (J = 15/2, 13/2)	545, 850	3100	0.7[c]
		$^4F_{9/2}$	$^4I_{15/2}$	660	2850	0.6[c]
		$^4I_{9/2}$	$^4I_{15/2}$	810	2150	4.5[c]
		$^4I_{13/2}$	$^4I_{15/2}$	1.54	6500	0.66 (0.7−12)
Tm	$^3H_6$	$^1D_2$	$^3F_4$, $^3H_4$, $^3F_3$, $^3F_2$	450, 650, 740, 775	6650	0.09
		$^1G_4$	$^3H_6$, $^3F_4$, $^3H_5$	470, 650, 770	6250	1.29
		$^3H_4$	$^3H_6$	800	4300	3.6[c]
Yb	$^2F_{7/2}$	$^2F_{5/2}$	$^2F_{7/2}$	980	10 250	2.0 (0.5−2.0)[f]

[a] G = ground state; I = main emissive state; F = final state; gap = energy difference between I and the highest SO level of F. [b] Values for the aqua ions,[43] otherwise stated, and ranges of observed lifetimes in all media, if available, between parentheses. [c] Doped in Y_2O_3 or in $YLiF_4$ (Ho), or in $YAl_3(BO_3)_4$ (Dy). [d] Luminescence from $^5D_1$, $^5D_2$, and $^5D_3$ is sometimes observed as well. [e] Luminescence from four other states has also been observed: $^4D_{5/2}$, $^2P_{3/2}$, $^4G_{11/2}$, $^2H_{9/2}$. [f] Complexes with organic ligands: 0.5−1.3 ms;[44,45] solid-state inorganic compounds: ≈2 ms.

"hypersensitive"; a typical example is Eu($^5D_0 \rightarrow {}^7F_2$). In general, transitions contain both ED and MD contributions.[41]

Important parameters characterizing the emission of light from a Ln^{III} ion are the lifetime of the excited state $\tau_{obs} = 1/k_{obs}$ and the quantum yield Q simply defined as:

$$Q = \frac{\text{number of emitted photons}}{\text{number of absorbed photons}} \quad (1)$$

The quantum yield is related to the rate k_{obs}, at which the excited level is depopulated and to the radiative rate constant k^{rad}:

$$Q_{Ln}^{Ln} = \frac{k^{rad}}{k_{obs}} = \frac{\tau_{obs}}{\tau^{rad}} \quad (2)$$

Subscript and superscript "Ln" are added to avoid confusion with another definition of quantum yield (see below). In fact, the quantity defined in eq 2 is the *intrinsic quantum yield*, that is, the quantum yield of the metal-centered luminescence upon direct excitation into the 4f levels. Its value reflects the extent of nonradiative deactivation processes occurring both in the inner- and outer-coordination spheres of the metal ion. The rate constant k_{obs} is the sum of the rates of the various deactivation processes:

$$k_{obs} = k^{rad} + \sum_n k_n^{nr} = k^{rad} + \sum_i k_i^{vibr}(T) + \sum_j k_j^{pet}(T) + \sum_k k'^{nr}_k \quad (3)$$

where k^{rad} and k^{nr} are the radiative and nonradiative rate constants, respectively; the superscript vibr points to vibration-induced processes, while pet refers to photoinduced electron transfer deactivation, generated, for instance, by LMCT states; the rate constants k' are associated with the remaining deactivation paths. In the absence of nonradiative deactivation processes, $k_{obs} = k^{rad}$ and the intrinsic quantum yield would be equal to 1, which is very rare except for some inorganic lamp phosphors.[42]

The intrinsic quantum yield depends on the energy gap ΔE between the emissive state of the metal ion and the highest sublevel of its receiving, multiplet. The smaller this gap, the easier is its closing by nonradiative deactivation processes, for instance through vibrational overtones of the bound ligands, particularly those with high energy (O−H, N−H, or C−H). Radiative de-excitation will compete efficiently with multiphonon processes if the energy gap is more than ≈6 quanta of the highest energy vibration present in the molecule. This type of nonradiative deactivation is especially detrimental to NIR luminescence:[24,39] for Er^{III} for instance, a C−H vibrator located at a distance between 20 and 30 Å from the emitting center induces a radiationless rate comparable to the radiative one.[46,47] Direct determination of the intrinsic quantum yield is difficult in view of the weak f−f absorptions so that it is usually estimated from eq 2, that is, evaluation of the radiative lifetime from Einstein's rates of spontaneous emission is required. This is by no means a trivial calculation.[18,24] Alternatively, if the absorption spectrum $\varepsilon(\tilde{\nu})$ to the emissive level is known, which may be the case when the luminescence transitions terminate onto the ground level, the radiative lifetime can be calculated from the following equation:

$$\frac{1}{\tau^{rad}} = 2303 \times \frac{8\pi c n^2 \tilde{\nu}^2 (2J+1)}{N_A (2J'+1)} \int \varepsilon(\tilde{\nu})\, d\tilde{\nu} \quad (4)$$

here N_A is Avogadro's number (6.023×10^{23}) and J and J' are the quantum numbers of the initial and final states, respectively. In the special case of Eu^{III} for which the $^5D_0$

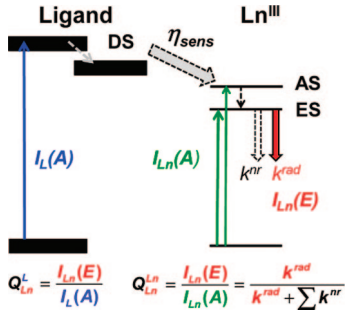

Figure 2. Simplified scheme depicting the definitions of Q^{L}_{Ln} and Q^{Ln}_{Ln}. DS = donor state, AS = acceptor state, ES = emitting state, A = absorption, E = emission; dotted arrows denote nonradiative processes.

$\rightarrow {}^7F_1$ transition has pure magnetic origin, a convenient simplified equation holds:[48]

$$A(\Psi_J,\Psi'_{J'}) = \frac{1}{\tau^{rad}} = A_{MD,0}\cdot n^3\left(\frac{I_{tot}}{I_{MD}}\right) \qquad (5)$$

with $A_{MD,0}$ being a constant equal to 14.65 s^{-1} and (I_{tot}/I_{MD}) the ratio between the total integrated emission intensity ${}^5D_0 \rightarrow {}^7F_J$ ($J = 0-6$) and the integrated intensity of the MD transition ${}^5D_0 \rightarrow {}^7F_1$.

It is important to stress that the radiative lifetime is characteristic of one emitting state; if several excited states emit light, then each of them will have a characteristic radiative lifetime. Moreover, the radiative lifetime is not constant for a given ion and a given electronic level (see the refractive index dependence in eq 5); transposition of a literature value to a specific compound cannot be made directly, as seen from the wide range of τ^{rad} values reported for an individual Ln^{III} ion (Table 1). Finally, τ^{rad} is sometimes estimated from τ_{obs} (77 K); here again, extreme care has to be exercised because, even at this temperature, nonradiative deactivations other than vibrations are still operating.

2.2. Sensitization by Organic Ligands

As stated above, sensitization of Ln^{III} luminescence by organic ligands is an intricate process, so it will not be discussed here; see refs 18, 24 for more details. An oversimplified scheme is given in Figure 2. When excitation is achieved through the ligand levels, the corresponding quantum yield is termed *overall quantum yield*, Q^{Ln}_{L}. It is related to the intrinsic quantum yield by the following equation:

$$Q^{Ln}_{L} = \eta^{D}_{pop}\cdot\eta_{et}\cdot Q^{Ln}_{Ln} = \eta_{sens}\cdot Q^{Ln}_{Ln} \qquad (6)$$

The two parameters in the middle term are (i) the efficiency η^{D}_{pop} with which the feeding level(s), ${}^1S$, ${}^3T$, ILCT, LMCT, ${}^3MLCT$, 4f5d states, is (are) populated by the initially excited state(s) and (ii) the efficiency of the energy transfer η_{et} from the donor state to the accepting Ln^{III} level. In some cases, particularly when the Ln^{III} ion is easily reducible (Sm^{III}, Eu^{III}, Yb^{III}), a redox-based mechanism can operate in which the first step is a photoinduced electron transfer to the Ln^{III} ion.[49] The overall sensitization efficiency, η_{sens} can be accessed experimentally if both the overall and intrinsic quantum yields are known or, alternatively, the overall quantum yield and the observed and radiative lifetimes:

$$\eta_{sens} = \frac{Q^{Ln}_{L}}{Q^{Ln}_{Ln}} = Q^{Ln}_{L}\cdot\frac{\tau^{rad}}{\tau_{obs}} \qquad (7)$$

The lifetime method is especially easy to implement for Eu^{III} compounds (see eq 5). Note that if the intrinsic quantum yield is directly proportional to τ_{obs}, this is not necessarily the case for the overall quantum yield because a change in the inner coordination sphere may influence η_{sens} through the resulting electronic changes in the molecular edifice. In the literature, the distinction between intrinsic and overall quantum yields is often unclear, particularly for NIR-emitting ions for which authors commonly rely on eq 2 for estimating Q^{Ln}_{Ln} with the help of a "literature" value for τ^{rad}, so that extreme care must be exercised in interpreting these data,[24,39] as shown by the determination of τ^{rad} by eq 4 for a series of Yb^{III} complexes.[45] As a result, few reliable determinations of η_{sens} are reported. On the other hand, systematic synthetic efforts during the past three decades have led to the identification of organic ligands providing large values of η_{sens} and, in the case of visible luminescence, minimizing nonradiative deactivation in the inner coordination sphere. Some examples are given in Table 2.

2.3. Information Gained from Lanthanide Luminescent Probes

Several quantitative structural, kinetic, and analytical parameters can be extracted by monitoring the luminescence of Ln^{III} ions inserted into an inorganic matrix or a molecular edifice.[18,61] Three of them are of particular relevance to biosciences: the hydration number q, resonant energy transfer, and luminescence quenching.

2.3.1. Hydration Numbers

Quenching of the lanthanide luminescence by high-energy vibrational overtones is a major concern in the design of luminescent probes. On the other hand, it allows one to assess the number of water molecules q interacting in the inner-coordination sphere from lifetimes measured in water and deuterated water. Several phenomenological equations have been proposed, based on the assumptions that O−D oscillators contribute little to deactivation and that all the other deactivation paths are the same in water and in deuterated water and can henceforth be determined by measuring the lifetime in the deuterated solvent. An important point for applying these equations is to make sure that quenching by solvent vibrations is by far the most efficient deactivation in the molecule. If other temperature-dependent phenomena (e.g., phonon-assisted back transfer or LMCT quenching) are operating, the relationships become unreliable. Altogether, such relationships, which exist for Nd^{III}, Sm^{III}, Eu^{III}, Tb^{III}, Dy^{III}, and Yb^{III}, are to be used with care and bearing in mind their peculiar calibration:

$$q = A\times(\Delta k_{obs} - B) - C \qquad (8)$$

$$\Delta k_{obs} = k_{H2O} - k_{D2O} = 1/\tau(H_2O) - 1/\tau(D_2O) \qquad (9)$$

where Δk_{obs} is expressed either in ms^{-1} or μs^{-1} depending on the ion; A, B, and C are phenomenological, Ln-depending (and sometimes ligand-depending) parameters determined using series of compounds with known hydration numbers.

Table 2. Photophysical Parameters of Highly Luminescent Tb^{III} and Eu^{III} Complexes with Organic Ligands[a]

complex	state	q	λ_{exc}/nm	Q^L_{Ln}	$\tau_{obs}(^5D_J)$/ms[b]	ref
$[Eu(tta)_3(DBSO)_2]$[c]	solid	0	370	0.85	0.71	50
$[Eu(\mathbf{L1})_3]$	solid	0	254	0.80	na	51
$[Eu(NO_3)_3(\mathbf{L2})_2]$	solid	0	336	0.70	1.31	52
$[Eu(\mathbf{L3})_3]$	solid	0	330	0.68−0.71	2.7−3.0	53
	CH_2Cl_2			0.51−0.52	2.7−2.8	
$[Eu(tta)_4]^-$	CH_3CN	0	360	0.63	na	54
$[Eu(\mathbf{L4})_3]$	CH_3CN	0	315	0.60	2.2	55
$[Tb(\mathbf{L5a})_3]$	solid	0	254	1.00	na	51
$[Tb(\mathbf{L6})]^-$	H_2O, pH 8.6	0	280	0.95	2.60	56
$[Tb(\mathbf{L5b})(H_2O)]$	solid	1	340	0.88	na	57
$[Tb(\mathbf{L7})_3]$	15% in PHB[d]	2	320	0.86	0.93	58
$[Tb_2(\mathbf{L8})(NO_3)_2(dmf)_6]$	solid	0	360	0.85	1.47	59
$[Tb(NO_3)_3(\mathbf{L2})_2]$	solid	0	336	0.80	1.70	52
$[Tb(H_2\mathbf{L9})_2]^+$	H_2O	n.a.	354	0.61	na	60

[a] See Chart 1 for ligand formulas; at room temperature; q = hydration number. [b] J = 0 and 4 for Eu^{III} and Tb^{III}, respectively. [c] DBSO = dibenzylsulfoxyde. [d] PHB = polyhydroxybutyrate.

Chart 1. Ligands Giving Highly Luminescent Eu^{III} and Tb^{III} Complexes (See Table 2)

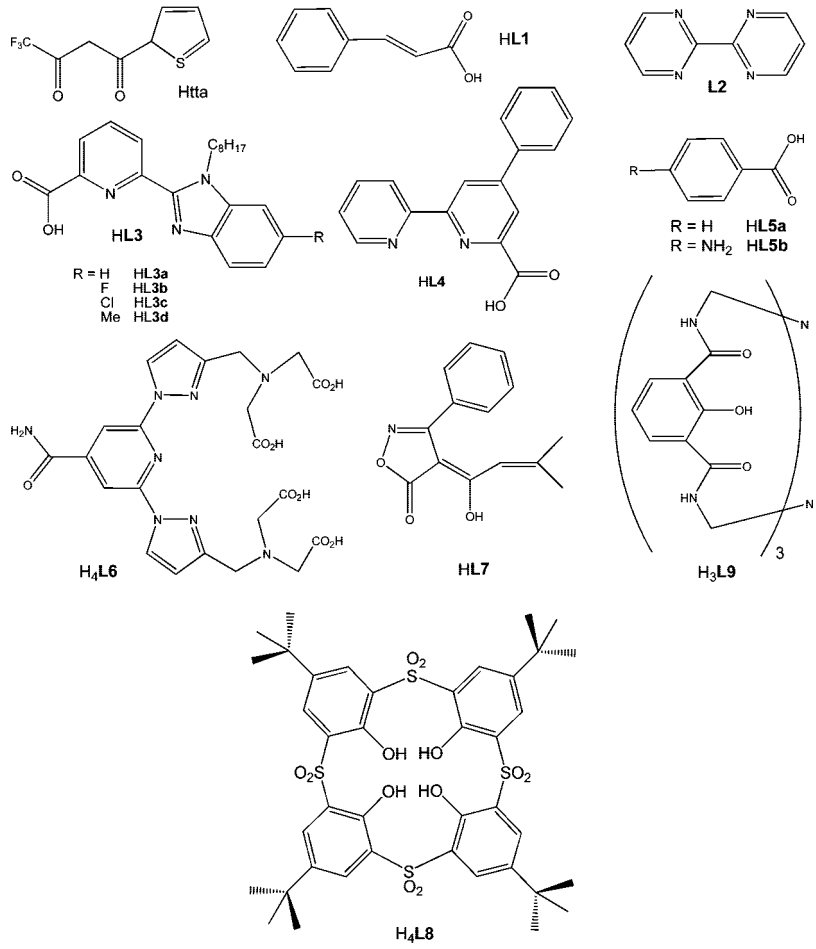

Parameter A describes the inner-sphere contribution to the quenching, parameter C the outer-sphere contribution of closely diffusing solvent molecules, while the corrective factor B, which has the same units as k, accounts for the presence of other deactivating vibrations in the neighborhood (e.g., N−H or C−H oscillators).[62] Alternatively, Δk_{obs} has sometimes been replaced by k_{H2O}. The resulting phenomenological equations are less reliable and have to be used with the same type of ligands because they imply that the vibrational deactivation by the ligand (taken into account by parameter C) is either negligible or at the least the same for the series of investigated chelates. Another practice to avoid is to use k_{77K} as k_{D2O} because this implies again that all nonradiative deactivation processes are switched off at this temperature, which is not necessarily the case. Relevant parameters are collected in Table 3.

2.3.2. Energy Transfer and FRET Experiments

If an accepting chromophore (A) lies in the vicinity of an excited luminophore, the latter may act as a donor (D) and transfer its energy onto the acceptor. The lifetime and the emission intensity of the donor decrease while the luminescence of the acceptor is switched on. The separation between

Table 3. Parameters for Phenomenological eqs 8 and 9 Allowing the Calculation of Lanthanide Hydration Numbers

Ln[a]	compd	measured parameter[a]	A	B	C	uncertainty on q	ref
Nd	9 polyaminocarboxylates in water	k_{H2O}, μs^{-1}	0.36	0	2.0	±0.4	63
Sm	9 polyaminocarboxylates in water	k_{H2O}, ms^{-1}	0.026	0	1.6	±0.5	64
Eu	9 polyaminocarboxylates in water	k_{H2O}, ms^{-1}	1.1	0	0.71	±0.5	64
Eu	12 crystalline solids + 6 complexes in water	Δk_{obs}, ms^{-1}	1.05	0	0	±0.5	65
Eu*	25 complexes in water	Δk_{obs}, ms^{-1}	1.11	0.31	0	±0.1	66
Eu*	26 cyclen chelates[b]	Δk_{obs}, ms^{-1}	1.2	0.25[c]	0	±0.3	62
Tb	9 polyaminocarboxylates in water	k_{H2O}, ms^{-1}	4.0	0	1.0	±0.5	64
Tb	10 crystalline solids + 6 complexes in water	Δk_{obs}, ms^{-1}	4.0	0	0	±0.5	65
Tb*	17 cyclen chelates[b]	Δk_{obs}, ms^{-1}	5.0	0.06[d]	0	±0.3	62
Dy	9 polyaminocarboxylates in water	k_{H2O}, ms^{-1}	0.024	0	1.3	±0.5	64
Yb*	14 cyclen chelates[b]	Δk_{obs}, μs^{-1}	1.0	0.20	0	±0.3	62

[a] Stars denote equations the use of which is recommended. [b] Including edta and dtpa chelates. [c] $B = 0.25 + 1.2n^{NH} + 0.075n^{CONHR}$ with n^{NH} and n^{CONHR} being the number of coordinated NH and CONHR groups, respectively. [d] $B = 0.06 + 0.09n^{NH}$.

the two chromophores is then accessible through the determination of the energy transfer efficiency within the frame of Förster's dipole−dipole mechanism:

$$\eta_{et} = 1 - \frac{\tau_{obs}}{\tau_0} = \frac{k_0}{k_{obs}} = \frac{1}{1 + (R_{DA}/R_0)^6} \qquad (10)$$

in which τ_{obs} and τ_0 are the lifetimes of D in presence and in absence of A, respectively, R_{DA} is the D−A distance, and R_0 is the critical distance for $\eta_{et} = 50\%$ transfer. The parameter R_0 depends on (i) an orientation factor κ having an isotropic limit of 2/3, (ii) the quantum yield Q_D of the donor (in absence of the acceptor), (iii) the refractive index n of the medium, and (iv) the overlap integral J_{ov} between the emission spectrum $E(\tilde{\nu})$ of the donor and the absorption spectrum $\varepsilon(\tilde{\nu})$ of the acceptor:

$$R_0^6 = 8.75 \times 10^{-25}(\kappa^2 \cdot Q_D \cdot n^{-4} \cdot J_{ov}) \qquad (11)$$

$$J_{ov} = \frac{\int \varepsilon(\tilde{\nu}) \cdot E(\tilde{\nu}) \cdot (\tilde{\nu})^{-4}\, d\tilde{\nu}}{E(\tilde{\nu})\, d\tilde{\nu}} \qquad (12)$$

If R_{DA} is known from crystal structure determination, eq 10 yields both η_{et} and R_0. Otherwise, calculation of R_0 has to make use of eqs 11 and 12. Typical values for R_0 are 8−15 Å for Ln−Ln, 20−30 Å for Ln−M(3d), and up to 100 Å for Ln−organic chromophore pairs. Initial experiments on energy transfer between lanthanide probes in biomolecules has allowed determination of the distance between Ca^{II} and Zn^{II} ions in proteins (substituted by Ln^{III} ions) as well as the distance between tryptophan chromophores and these metal-ion sites.[67]

A more common application of directional energy transfer is Förster resonant energy transfer (FRET) analysis. It is used either in simple bioanalyses or to detect protein interactions, DNA hybridization, or conformational changes.[68] Its principle is shown in Figure 3. The dynamic of the energy migration in the system depends on the relative deactivation rate constants of the donor and the acceptor as well as on the transfer rate constant.

Two limiting cases can be distinguished. If $k_{obs}^D = k^D + k_{et}^{A,D} \gg k^A$, then the observed decay rate of the acceptor in presence of energy transfer is simply $k_{obs}^A = k^A$. On the other hand, if $k_{obs}^D = k^D + k_{et}^{A,D} \ll k^A$, then the lifetime of the acceptor is controlled by the donor and $k_{obs}^A = k_{obs}^D$. For instance, energy transfer from long-lived Cr^{III} to NIR-emitting Ln^{III} ions with short lifetimes (Nd^{III}, Yb^{III}) allows one to shift the apparent lifetime of the lanthanide ions into the ms range.[28,69] In analytical applications, the lengthening of the acceptor lifetime makes time discrimination of the acceptor emission possible, boosting the signal-to-noise ratio. The advantage of FRET combined with lanthanide luminescent probe technology is to eliminate the need for washing unreacted reagents because the transfer only occurs when the two entities, the lanthanide donor and the organic acceptor, are linked together via some kind of conjugation. Recent developments include combining quantum dots (QDs) and lanthanide chelates for very large distance FRET experiments displaying improved sensitivity.[70,71] Despite their inherent disadvantages (see Introduction) the plus brought by QDs is the easy tuning of R_0: increasing the QD core size leads to a bathochromic shift of the emission spectrum, so that J_{ov} may be maximized (see eq 11). Combining them with lanthanide chelates results in FRET transfer to the QDs, a process which is sometimes difficult when the donor is an organic fluorophore, even if the D−A distance is favorable. An explanation put forward evokes a mismatch between the lifetimes of the donor and QDs.[72]

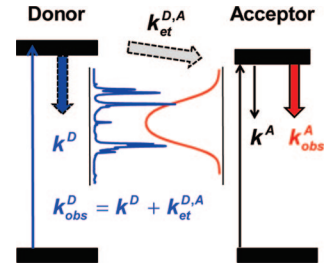

Figure 3. Principle of Förster resonant energy transfer (FRET).

2.3.3. Collisional (Stern−Volmer) Quenching

Interaction between a luminescent stain and molecules present in solution results in luminescence quenching and quantitative investigation of the phenomenon provides both analytical and photophysical information. In collisional (dynamic) quenching, the quencher molecule Q diffuses toward the luminescent probe during the lifetime of its excited state; upon collision, the excitation energy is dissipated nonradiatively. The average distance that a molecule having a diffusion coefficient D can travel in solution during the lifetime of the excited state is given by:

$$\bar{x} = \sqrt{2D\tau_{obs}} \qquad (13)$$

A common collisional quencher is molecular oxygen which has a diffusion coefficient of 2.5×10^{-5} $cm^2 \cdot s^{-1}$ in water at 298 K. During the lifetime of a Ln^{III} excited state

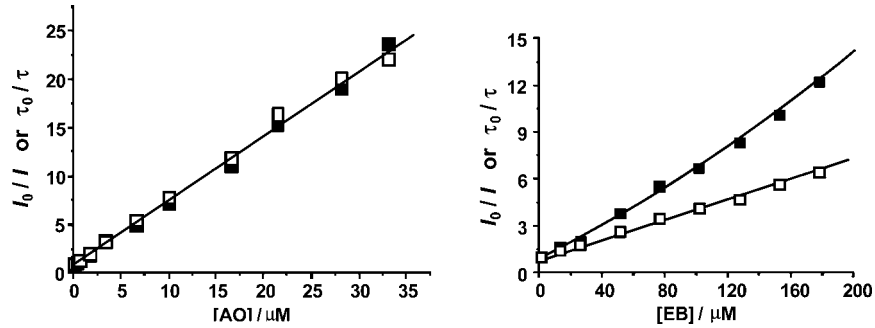

Figure 4. Stern−Volmer plots for the quenching of the luminescence of $[Eu_2(\mathbf{43b})_3]$ by acridine orange (left) and ethidium bromide (right) in Tris-HCl buffer (pH 7.4). Open squares: lifetimes; solid squares: intensities. (Redrawn after ref 74. Copyright Royal Society of Chemistry.)

such as $Eu(^5D_0)$ or $Tb(^5D_4)$, typically 1 ms, it can therefore diffuse over 2.2 μm, that is a distance comparable to the size of a biological cell. In some instances, a nonluminescent complex may result from the collision (static quenching). Otto Stern and Max Volmer have worked out the corresponding equations.[73] For dynamic quenching:

$$\frac{I_0}{I} = 1 + K_D[Q] = 1 + k_q\tau_0[Q] \qquad (14)$$

in which K_D is the dynamic quenching constant, k_q the bimolecular rate constant, I_0 and I the emission intensities in the absence and in the presence of quencher, respectively, and τ_0 the observed lifetime in absence of quencher. When collisional quenching occurs, the lifetime decreases in parallel to the luminescence intensity:

$$\frac{I_0}{I} = \frac{\tau_0}{\tau} \qquad (15)$$

A similar equation can be derived for static quenching, with K_S being the static quenching constant:

$$\frac{I_0}{I} = 1 + K_S[Q] \qquad (16)$$

When both dynamic and static quenching occurs, the equations combine into:

$$\frac{I_0}{I} = (1 + K_D[Q]) \cdot (1 + K_S[Q]) \qquad (17)$$

$$\frac{I_0}{I} - 1 = (K_D + K_S)[Q] + K_D \cdot K_S[Q]^2 \qquad (18)$$

Here again, eq 15 holds and luminescence intensities may be substituted with lifetimes. If the Stern−Volmer plot is linear, it reflects the sole presence of dynamic quenching. This is for instance the case for the quenching of the bimetallic $[Eu_2(\mathbf{L43b})_3]$ helicate (see Chart 12, section 5.4) with acridine orange (AO), as shown in Figure 4. This quenching has been taken advantage of to develop a versatile and robust method for the detection of various types of DNAs and of polymerase chain reaction (PCR) products (see section 4.5 below).[74] On the other hand, quenching of the same chelate with ethidium bromide (EB) is typical of both dynamic and static quenching.

2.4. Designing Efficient Lanthanide Luminescent Bioprobes (LLBs)

Efficient lanthanide luminescent bioprobes must meet several stringent requirements, both chemical, photophysical, and biochemical. The first two aspects include: (i) water solubility, (ii) large thermodynamic stability at physiological pHs and in presence of biological fluids, (iii) kinetic inertness, (iv) intense absorption above 330 nm to minimize destruction of live biological material and to maximize the $\varepsilon(\lambda_{exc})\cdot Q_L^{Ln}$ product, (v) efficient sensitization of the metal luminescence (η_{sens}), (vi) embedding of the emitting ion into a rigid, protective cavity minimizing nonradiative deactivation (Q_{Ln}^{Ln}), (vii) long excited state lifetime for TRD capability (τ_{obs}), and (viii) photostability. Biochemical requirements depend on how the experiments are conducted, in vitro or in vivo. With respect to the former, (ix) noncytotoxicity is required and often (x) ability of interacting specifically with the biological target while not altering the bioaffinity of the host (see section 3). For in vivo experiments, the matter of toxicity (and therefore thermodynamic stability and kinetic inertness) is highly critical, as well as (xi) the ability of the probe to be excreted in a reasonable span of time (typically 12−48 h).

Regarding stability, polydentate ligands are a must in order to benefit from a large entropic effect. In vivo experiments require pLns > 20 ($pLn = -\log[Ln^{III}]_{free}$ in water, at pH 7.4, $[Ln^{III}]_t = 1$ μM, and $[Ligand]_t = 10$ μM),[75] which severely limits the number of suitable ligands; carboxylates of cyclen derivatives and cryptates seem to be the best ones for the time being, while dtpa chelates are at the lower limit of the desired stability. For in vitro experiments, carboxylates,[76] aminocarboxylates,[56,77] phosphonates,[78,79] hydroxyquinolinates,[80,81] and chelates with hydroxyisophthalamide[11,60,82] are good candidates as well as self-assembled binuclear triple helical carboxylates,[15] while β-diketonates which have excellent photophysical properties[83] have the tendency to be less stable, particularly in aqueous solutions.[84]

The photophysical requirements are related to the two parameters in the right member of eq 6. The sensitization efficiency is difficult to master in view of the intricate processes going on. Phenomenological rules have nevertheless been established based on the simplistic model that the main energy transfer path implies the ligand triplet state and that the only parameter of importance is the energy gap between this state and the emitting Ln^{III} level. The following conclusions can be drawn from systematic studies published to date for Eu^{III} and Tb^{III}:[77,82,85−87]

(a) The maximum values of the quantum yields are usually recorded when the triplet state energy is close to the energy

of one of the higher excited states of the metal ion, consistent with the fact that the emissive level is usually not directly fed by the ligand excited states (Figure 2). However, when the energy of the feeding state becomes closer to the energy of the emitting state, back-energy transfer operates and the quantum yield usually goes down: a "safe" energy difference minimizing this process and optimizing the energy transfer is around 2500−3500 cm^{-1}.

(b) Quantum yields for Tb^{III} chelates tend to be larger compared to Eu^{III} (Table 2); although only very few determinations of Q_{Tb}^{Tb} and η_{sens} have been performed for Tb^{III}, this undoubtedly does not reflect a better energy transfer but, rather, the smaller Eu($^5D_0-^7F_6$) energy gap, 12800 cm^{-1} compared to Tb($^5D_4-^7F_0$), 14800 cm^{-1}, so that $Q_{Tb}^{Tb} > Q_{Eu}^{Eu}$ if the same coordination environment is considered.

Optimization of Q_{Ln}^{Ln} is easy to control in that one simply has to minimize deactivation by vibrational overtones of coordinated ligands. Recently, however, attention has been drawn on the radiative lifetime, see eq 2, because a shorter lifetime would mean a larger intrinsic quantum yield. It has been pointed out that highly emissive complexes of Eu^{III},[53] Tb^{III},[58] and Yb^{III}[45] all have short radiative lifetimes, rendering the emission more competitive with respect to nonradiative deactivation. Theoretically, the reason is simple: more orbital mixing leads to less pure 4f levels, relaxing the selection rules. However, a relationship between the radiative lifetime and the coordination environment in the chelates remains to be found.

3. Lanthanide Bioconjugates

A growing number of bioanalyses require specific targeting of the analyte, and therefore the lanthanide luminescent probes have to be fitted with adequate functionalities able to couple with biological material. The coupling is achieved either directly, e.g., in immunoassays in which the lanthanide probe is linked to a monoclonal antibody mAb, or indirectly, with the chelate being covalently bound to avidin (or biotin), and the resulting duplex being then fixed onto a biotinylated (or avidin derivatized) mAb via the strong avidin−biotin interaction (log $K \approx 10^{15}$).[88] Alternatively, avidin may be substituted by streptavidin[89] or bovine serum albumin (BSA).[90] Examples of indirect and direct coupling are depicted in Figure 5. The top part (a−c) shows the formation of the luminescent chelate by reaction of a ligand fitted with a chelating, a chromophoric, and a linking group, followed by its covalent coupling to avidin. The bottom part (d−e) describes the formation of the bioconjugate with a biotinylated monoclonal antibody (mAb) and the detection of a biomarker expressed by a live cell, as an example of a specific immunocytochemical reaction; a direct linking of the lanthanide label to the mAb is also illustrated (Figure 5e).

Covalent coupling of a lanthanide luminescent chelate to bioactive molecules such as proteins, nucleic acids, or peptides relies on the presence of chemically reactive groups on these molecules. The most common ones are aliphatic α- or ε-amines. The latter are typical of the amino acid lysine, the pK_a of which is 9.2 so that lysine reacts easily and cleanly above pH 8 to yield stable covalent binding. Moreover, there are usually several lysine groups per protein; for instance, avidin, which is a tetrameric protein present in egg white and which has a molecular weight of ≈67 kDa, bears 36 of them. The α-amino group is more acidic with pK_a around 7,

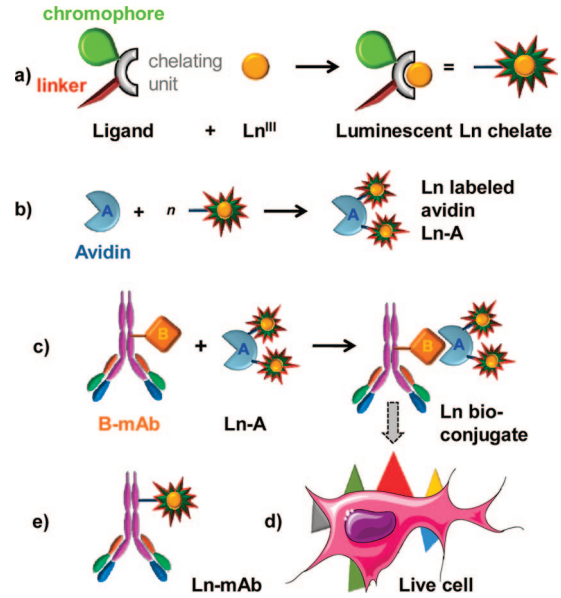

Figure 5. Schematic representation of (a) the formation of a luminescent lanthanide chelate, (b) its linking to avidin (A), (c) subsequent conjugation to a biotinylated monoclonal antibody (B-mAb), (d) recognition of a biomarker expressed by a live cell, as an example, and (e) a monoclonal antibody labeled with a luminescent lanthanide chelate.

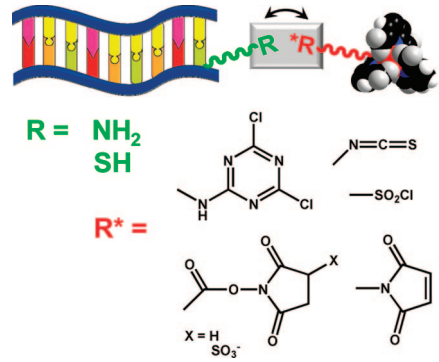

Figure 6. Typical reacting groups during bioconjugation of a lanthanide chelate: R is the residue on the protein while R* is the activated group on the lanthanide chelate.

and each protein bears at least one such group per subunit or peptide chain.

Thiol residues are other common reactive groups. The free thiol group (e.g., in cysteine) is more nucleophilic than amines and generally is the more reactive group in proteins, even at neutral pH. Phenol (e.g., in tyrosine) or carboxylic acids (e.g., in aspartic and glutamic acids) are other potential candidates.

To couple with all these functionalities, the lanthanide chelate is first activated. Here again, several routes using different functions are possible, the main one being depicted in Figure 6.

In immunoassays, coupling between proteinic amines and lanthanide chelates fitted with isothiocyanato, chlorosulfonyl (particularly arenesulfonyl), or 2,4-dichloro-1,3,5-triazinyl groups proved to be the most successful, the latter being more efficient than isothiocyanate.[19] Another very convenient coupling group is *N*-hydroxysuccinimide (NHS, or its sulfo derivative, sulfo-NHS), which can be easily generated by direct reaction of a carboxylic acid with *N*-hydroxysuccinimide in the presence of the dehydrating agent, 1-ethyl-3-(3-dimethylaminopropyl) carbodiimide hydrochloride (EDC

or EDAC, or EDCI). Because proteins bear several coupling functions, the number of attached LLBs may be large (up to 46).[8] Bioaffinity assays for diagnosis are gaining in interest so that numerous lanthanide bioconjugates have been synthesized. However, a large fraction of them are described in patent literature. The field has been reviewed recently[8] and remains quite vivid, with new chelators/sensitizer systems being proposed constantly. One recent example is the Eu^{III} chelate with 6,9-dicarboxymethyl-3-{4-([1,10]-phenanthrol-2-ylethinylphenyl-carbamoyl)-methyl}-3,6,9-triaza-)-undeca-1,11-dicarboxylic acid, which can easily be coupled to several proteins and yields highly sensitive time-resolved luminescence analyses, with detection limits of 1.5 fmol for BSA, 100 amol for lysozyme, and linear ranges of over 5 orders of magnitude.[91]

Bioconjugation of luminescent probes incorporated into nanoparticles (NPs)[92] or of quantum dots[93] is also feasible and has been attempted for lanthanide probes as well.[94−96] It is interesting to note that nanoparticles, if charged as is the case for silica NPs which bear negative charges, need not necessarily to be covalently linked to the biological molecule: electrostatic interaction between silica NPs and positively charged avidin is strong enough to generate a stable bioconjugate.[92]

Lanthanide ions also bind oligonucleotides,[97,98] and the resulting bioconjugates have been provided in the monitoring of hybridization reactions and phosphodiesterase activity by FRET technology.[99−101] Another way of targeting specific biomolecules or regions of biomolecules is to decorate peptides with lanthanide chelates through polyaminocarboxylate coordination.[102,103] For instance, to understand the fate of proteins in vivo, B. Imperiali and co-workers have developed several LLBs in which the luminescent lanthanide ion is linked to a small, genetically encoded protein fusion partner. This partner contains sensitizer moieties strategically located on the residue for efficient energy transfer. Typically, tryptophan (trp) is used for sensitizing Tb^{III} upon excitation at 280 nm, while acridone (acd) is an efficient chromophore for Eu^{III} under excitation at 390 nm. Carbostyril 124 (cs124) sensitizes the luminescence of both Eu^{III} and Tb^{III} upon excitation at 337 nm.[104] A typical sequence of peptides developed for strong Ln^{III} binding is H_2N-FITDNNDGX-IEGDELLLEEG-$CONH_2$ in which the amino acid labeled X bears the chromophore (trp, acd, or cs124). With standard laboratory equipment, these tags display comparable sensitivity as Coomassie blue but application of TRD detection is expected to largely lower the limit of detection of the LLB-tagged proteins.

4. Bioanalyses with Lanthanide Luminescent Probes

Most luminescent sensors operate in water, and two types can be distinguished.[12,105−108] In the first one, the sensor is immobilized, for instance in silicon thin layers directly integrated into an electronic readout circuit, or in sol−gel glasses, for instance for flow-injection analysis. The second type of sensors involves classical luminescent probes in solution for in vitro and/or in vivo applications. In this case, the emitted signal has to be ratioed to another signal to avoid concentration dependence (so-called ratiometric method). The current trend in biosensors is to develop more sensitive probes based on nanostructures[109] and to exploit the time-resolved capability of lanthanide luminescent bioprobes.

Chart 2. Chelating Molecules for Luminescent Lanthanide Biolabels Used in Heterogeneous Immunoassays

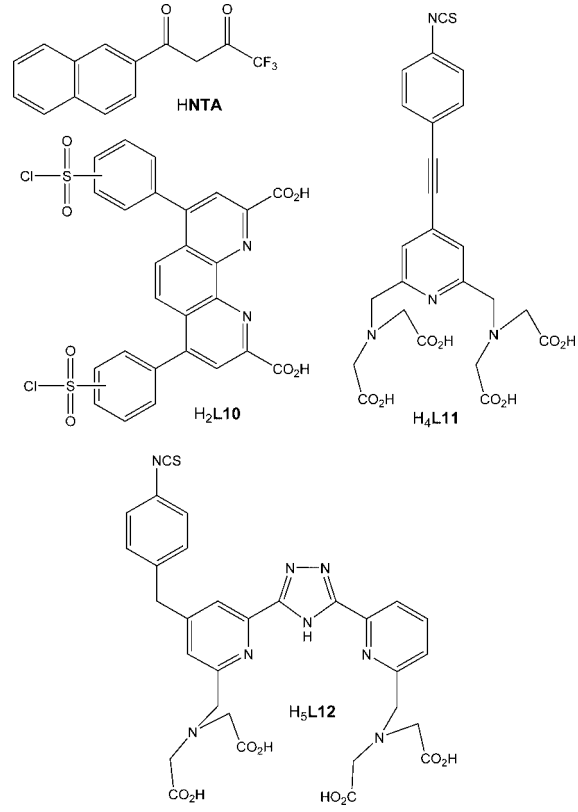

4.1. Heterogeneous Immunoassays

Time-resolved detection was applied to these assays in view of the many undesirable substances coexisting in blood serum or in urine. Two lanthanide chelates are used in the initial analysis format, the so-called "heterogeneous immunoassays", which were commercialized under the name dissociation-enhanced lanthanide fluorometric immunoassay (DELFIA).[110] The analyte is first linked to a specific binding agent immobilized on a solid support. After this step, another specific immunoreaction couples a poorly luminescent lanthanide complex with the analyte and the unreacted reagents are washed out. The chelate is then dissociated in acidic medium and converted into another, highly luminescent complex protected by a micelle thanks to an enhancement solution. Subsequent time-resolved detection of the metal-centered luminescence yields the desired analytical signal. Antigens (e.g., hepatitis B surface antigen), steroids (e.g., testosterone or cortisol), as well as hormones (e.g., thyrotropin or luteotropin) are routinely assayed with this heterogeneous technique. The enhancement solution usually contains an aromatic β-diketonate (e.g., NTA^-, Chart 2), trioctylphosphine oxide, and Triton X-100. The principle is sketched in Figure 7 in which the lanthanide chelate is shown as being directly bound to the antibody, but sensitivity enhancement of the assays may be gained by multilabeling of the monoclonal antibody with the biotin−avidin technique, much as shown in Figure 5. Another way of increasing the luminescence signal is to resort to columinescence enhancement by adding a nonluminescent ion (usually Y^{III}) in the solution; the corresponding chelate absorbs light and excites the luminescent complexes par collisional transfer.[110,111] Enhancement factors in the range 200−800 are routinely obtained, boosting the limit of detection (LOD) to 10^{-14} M.

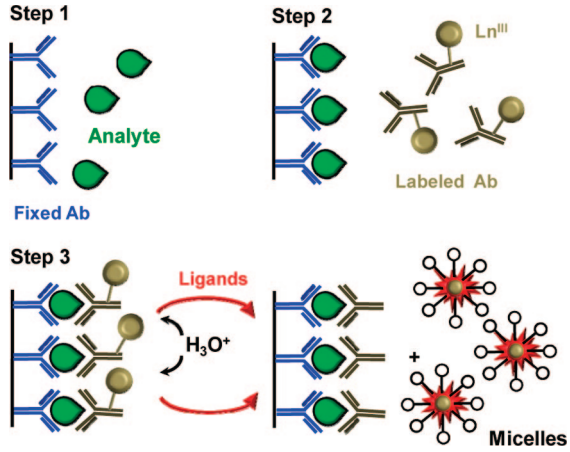

Figure 7. Principle of an heterogeneous luminescent immunoassay (Ab = antibody): fixation of the analyte (step 1), immunochemical reaction with the labeled antibody (step 2), release of Ln^{III} followed by complexation and insertion into micelles (step 3).

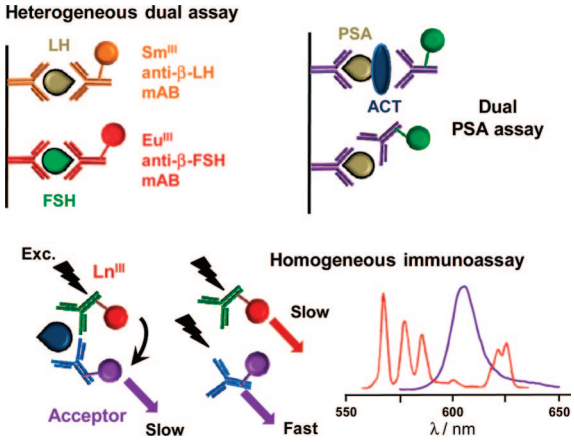

Figure 8. (Top left) Heterogeneous dual assay of luteinizing (LH) and follicle stimulating (FSH) hormones with $Sm^{III}$and Eu^{III}bioconjugates.[111] (Top right) Dual assay of free and bound PSA.[112] (Bottom left) Principle of an homogeneous immunoassay showing time (slow/fast) and spectral discrimination of the unreacted monoclonal antibodies. (Bottom right) emission spectra of $[Eu(\mathbf{L14})]^-$ (see Chart 3) in red and of XL665 in violet.

An interesting development is the design of dual-label assays, one example of which is the simultaneous detection of luteinizing (LH) and follicle stimulating (FSH) hormone (Figure 8, top left). The corresponding monoclonal anti-β-LH and anti-β-FSH antibodies are labeled with Eu^{III} (3.8 labels per molecule) and Sm^{III} (26 labels per molecule), respectively, and the assay is carried out as sketched in Figure 7. The larger number of Sm^{III} labels per molecule compensates the much smaller quantum yield of luminescent Sm^{III} chelates compared to Eu^{III} ($\approx$10-fold) so that similar limits of detection are obtained (0.03−0.05 international units (IU) per liter).[111]

Improvements of these initial protocols came in two ways. First, the two lanthanide chelates were replaced by a single luminescent complex. In the CyberFluor protocol, the luminescent chelate, for instance $[Eu(\mathbf{L10})]^+$ (see Chart 2), is conjugated to the mAb, and its luminescence is detected on the surface of the solid support used for immobilization.[113]

Dual assays have soon benefited from this improvement and a landmark in the field is the one-step dual assay of free and bound prostate specific antigen (PSA), the concentration of which increases in prostate cancer patients (Figure 8, top right).[112] PSA, a glycoprotein, is present in the blood plasma,

Chart 3. Cryptand for Homogeneous Luminescent Immunoassays[121]

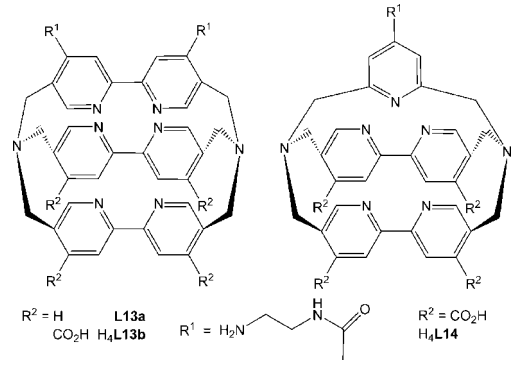

either under its free form or bound to serine protease inhibitor α_1-antichymotrypsin (ACT). The monoclonal antibody recognizing solely free PSA is labeled with $[Eu(\mathbf{L11})]^-$, while the monoclonal antibody recognizing both free and bound forms is labeled with $[Tb(\mathbf{L12})]^{2-}$ (Chart 3). Free PSA and bound PSA-ACT are first bound to the immobilized mAb recognizing both: the labeled antibodies are then added, and after incubation and washing, a buffer solution is added which dissociates the labeled mAbs; finally, the luminescence of Eu^{III} and Tb^{III} is measured in the same solution.[112,114] Limits of detection are on the order of 0.01 ng/mL for free PSA and 0.1 ng/mL for bound PSA. Similar tests have recently been developed, which take advantage of nanoparticles: surface-modified Tb-containing silica nanoparticles[115] or streptavidin-coated Eu-containing polystyrene nanoparticles coupled with avidin−biotin and microarray analysis technologies.[116,117] Limits of detection can be increased up to 50-fold,[116] and the dynamic range of the assay is much larger.

Heterogeneous assays have the disadvantage of necessitating elimination of unreacted labeled mAbs before reading the luminescence signal, which implies numerous washing phases. However DELFIA is still widespread and new applications are burgeoning. For instance, J. Hovinen et al. have recently proposed to improve the detection of point mutations in DNA (a method called minisequencing) of cystic fibrosis. Four different acyclic nucleoside triphosphates have been labeled with nonluminescent Ln chelates (Ln = Sm, Eu, Tb, Dy). Thirty-two blood spot samples were used for PCR amplification (without DNA isolation), and the target mutations have been genotyped by time-resolved luminescence detection after application of the enhancer solution. One- and two-label assays performed best, while the four-label assay still needs optimization, particularly at the PCR step.[118]

A second substantial improvement to heterogeneous assays consists in using FRET capability to overcome this shortcoming, as described in the next section.

4.2. Homogeneous Immunoassays

Homogeneous assays (sometimes referred to as HTRF, homogeneous time-resolved fluorescence) rely on direct modulation of the label luminescence during the biochemical reaction under scrutiny. The antigen of interest is coupled to two mAbs, one decorated with a lanthanide label and the other one with an organic acceptor emitting at a wavelength distinct from the Ln^{III} emission (Figure 8, bottom). After completion of the immunoreactions, the sample is illuminated

by UV light and four types of luminescence develop: (i) two fast decaying signals, background autofluorescence and fluorescence from the organic conjugate not bound to the antigen, and (ii) two slow decaying emissions, phosphorescence from the lanthanide conjugate not bound to the antigen (as well as residual luminescence from the bound one) and emission from the organic acceptor bound to the antigen and excited through FRET (see section 2.3.2). Measurement in time-resolved mode allows one to eliminate the fast decaying luminescence signals while spectral discrimination isolates the sought for signal from the organic acceptor fed by the FRET process. In this way, removal of the unreacted conjugates is not necessary and the analysis time is reduced substantially, making this technique, initially proposed by L. E. Morrison,[119,120] adequate for high throughput screening operations.[7] TR homogeneous assays have been commercialized under the trademarks homogeneous time-resolved fluorescence (HTRF) and time-resolved amplification of cryptate emission (TRACE) from CisBio International, or Lanthanide chelate energy transfer (LANCE) from PerkinElmer, Lanthascreen from Invitrogen, among others. We do not intend to review all these technologies and only describe a few examples.

The luminescent chelate used for the CisBio assays is an europium tris(bipyridine) cryptate (see Chart 3) with large thermodynamic stability and presenting the advantage over nonmacrocyclic chelates that its dissociation is extremely slow. Indeed, the corresponding transition state implies that one bridgehead nitrogen changes conformation and has its lone pair pointing outward, which results in a high activation energy ($\Delta G^* \approx 100-120$ kJ·mol^{-1}). Thanks to the robustness of the macrocyclic edifice, harsh experimental conditions, such as those prevailing during peptide synthesis or reverse phase chromatography in the presence of trifluoroacetic acid, can be used without destroying the complex. The development of a suitable luminescent cryptate is an interesting case study of ligand optimization. In fact, if the initial chelate, [Eu(**L13a**)]$^{3+}$ (Chart 3, $Q^L_{Eu} = 2\%$), retains its photophysical properties upon bioconjugation (e.g., to IgG), the macrocyclic cavity is somewhat too large for Eu^{III} ions, the coordination sphere of which is not saturated and can take up two water molecules.[121] This is of course detrimental to the emissive properties and has to be overcome by the addition of fluoride anions which strongly bind lanthanide ions and therefore substitute water. Another drawback is its relatively short excitation wavelength, 307 nm. Adding four carboxylic acid functions to the cryptand (H$_4$**L13b**) remedies to some of these disadvantages, in particular, the excitation wavelength is red-shifted by 17 nm, so that a nitrogen laser can be used as excitation source. However, aromatic amines generate LMCT states which easily quench the Eu^{III} luminescence[122,123] and [Eu(**L13b**)]$^-$ is still relatively weakly luminescent. Because the process leads to the formation of the much larger Eu^{II} ion in the excited state ($r_i = 1.30$ Å versus 1.12 Å for Eu^{III}), replacement of one bipyridine by pyridine solved this problem: the smaller cavity destabilizes the divalent europium intermediate. The resulting [Eu(**L14**)]$^-$ cryptate is sufficiently luminescent ($Q^{Ln}_L \approx 7-10\%$) for highly sensitive analyses and for not requiring the use of cytotoxic fluoride.

The organic acceptor is a derivative of a protein-pigment found in the phycobilisomes of red algae, located in the thykaloid membrane of the cells. Its role is to absorb light involved in photosynthesis (620 nm) and to funnel its energy into the photosystem of the cell. One element of the phycobilisomes is allophycocyanin, a 105 kDa trimeric phycobiliprotein absorbing between 600 and 660 nm and emitting at 665 nm with a quantum yield of 68% (Figure 8, bottom right). It has a high molar absorptivity ($\varepsilon \approx 7.3 \times 10^5$ M^{-1} cm^{-1}) and the yield of FRET from Eu^{III} is 75% and 50% for $R_{DA} = 7.5$ and 9 nm, respectively.[124] Because the trimeric structure is required for retaining these photophysical properties, the natural protein is cross-linked between its α and β subunits, yielding the so-called XL665 acceptor dye. Alternatively, simpler NIR-emitting dyes can function as energy acceptors, e.g. Alexa Fluor 647 ($\varepsilon_{650} = 2.4 \times 10^5$ M^{-1} cm^{-1}).[125]

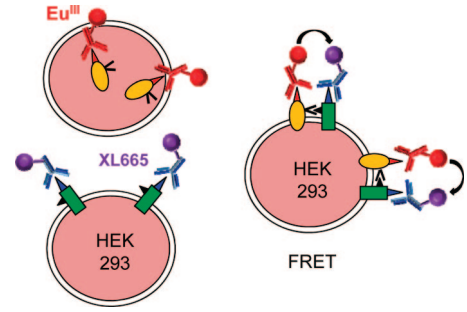

Figure 9. (Left) Recognition of the two GABA$_B$ subunits by different labeled antibodies. (Right) FRET signaling the presence of the dimer expressed on the cell membrane.[125]

Analyses are performed in ratiometric mode: the emission signal of XL665 at 665 nm is ratioed against the signal of the Eu^{III} cryptate at 620 nm ($^5D_0 \rightarrow {}^7F_2$ transition), yielding a measurement independent of the optical characteristics of the sample at the excitation wavelength and freeing the analysis of any inner-filter effect.

An example of such an analysis is the visualization of membrane protein interaction at the surface of living cells (HEK 293) by evidencing the γ-butyrate receptor B (GABA$_B$).[125] This receptor forms dimers composed of two GABA$_B$ subunits, GABA$_{B1}$ and GABA$_{B2}$. The GABA$_{B1}$ receptor is retained in the endoplasmatic reticulum (ER) when expressed alone. The GABA$_{B2}$ unit, which activates green fluorescent protein (GFP),[126] releases GABA$_{B1}$ from the ER and allows expression of the heterodimer on the surface of the cells. The two receptors bear tags which are recognized by specific antibodies, one of which is labeled with the organic acceptor and the other with the Eu^{III} cryptate. When the dimer forms at the membrane surface, FRET develops and the NIR luminescence of XL665 (or another suitable organic dye) is measured in time-resolved mode (Figure 9). A sensitivity of 10 fmol per well has been achieved.

The first-generation HTRF technology was extended recently by the introduction of a Tb^{III} cryptate with a receptor featuring three 2-hydroxyisophthalamide chelating units linked by two amine bridgeheads (H$_3$**L9**, Chart 1), which is much more luminescent than the Eu^{III} cryptate, with a quantum yield of ≈60%.[60] FRET experiments with Tb^{III} usually requires different acceptors than when Eu^{III} is the donor, but here the Tb^{III} cryptate is compatible with the same acceptor dyes as the Eu^{III} cryptate. In addition, the Tb^{III} cryptate can also transfer energy onto green-emitting fluorophores, such as GFP, which enlarges its applicability because this protein can be fused directly to the target molecules.[127]

The FRET technology and, to a lesser extent, heterogeneous immunoassays, have opened wide perspectives in

Chart 4. Nonadentate Ligands for Europium and Terbium Labels Used in Point-of-Care Immunoassays and Automated PCR Platform

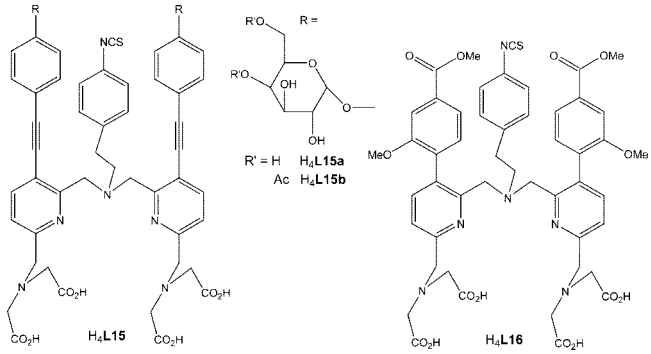

biosciences and have been successfully applied in time-resolved luminescence flow cytometry,[128,129] DNA hybridization assays,[130] detection of enzyme activity,[131] real-time polymerase chain reactions (PCR),[132] and genotyping,[118] to name a few.

For instance, a PCR platform for small-scale analysis of nucleic acids combines a PC-controlled thermal cycler with a time-resolved luminescence spectrometer. The homogeneous assays are performed with europium and terbium chelates with nonadentate ligands, e.g., [Eu(**L15**)]$^-$ developed for point-of-care immunoassay of human chorionic gonadotropin,[133] and [Tb(**L16**)]$^-$ (Chart 4). In the Eu-chelate, the α-galactose side groups ensure sufficient water solubility, facilitating coupling of the isothiocyanato group to antibodies. The entire procedure is made automatic in that it is conducted in plastic vessels containing all the necessary reagents under dry form; the vessels bear a barcode which after detection enables the software to perform the necessary operations. In this way, contamination is avoided. Moreover, an internal amplification control is included to prevent false positive. The limit of detection is as low as 20 pM for both lanthanide labels, with a dynamic range reaching 4 orders of magnitude. The platform is commercialized under the name GenomEra, and it is hoped it will help rendering PCR assays more reliable, faster, and cheaper.[132]

4.3. Up-Converting Phosphors and/or Nanoparticles

Up-converting phosphors (UCPs) or nanoparticles (UCNPs) are rare-earth doped ceramic-type materials such as oxides, oxysulfides, fluorides, or oxyfluorides which convert red into visible light. They are usually synthesized as micro- or nanospheres and were introduced as probes for bioassays in the 1990s. Most of them contain Er^{III} ions as two-color (green, 540 nm; red, 654 nm) emitters and Yb^{III} ions as sensitizers, but other Ln^{III} pairs have also been proposed (e.g., Tm^{III}/Ho^{III}). UCPs present several advantages over classical bioprobes, including high sensitivity, multiplexing ability if several different Ln^{III} ions are codoped, low sensitivity to photobleaching, and cheap laser diode excitation, in addition to deep penetration of the excitation NIR light. Initially, they have been used in luminescent immunoassays, but presently, their applications have been extended to luminescence imaging of cancerous cells;[134] novel imaging systems based on UCPs have been designed[135] and sensitivity down to single molecule detection within cells is foreseen.[136] The usefulness of UCPs in biological and medicinal analysis is summed up in recent review articles.[24,137,138]

4.4. Determination of Enzyme Activity

Screening tools for the development of new cancer therapies are in high demand and often require the determination of enzyme activities. Similarly, evidencing cell apoptosis is crucial for evaluating the effectiveness of the therapy; this process is intricate and involves several intracellular modulators which have to be detected. The great sensitivity and versatility of luminescence, particularly of time-gated luminescence, revealed to be ideal for this type of analysis and, in effect, this technique has recently become the most frequently used method in drug screening.

There are several ways of conducting the analysis, e.g. from the use of fluorogenic enzyme substrates, substrates bearing donor/acceptor groups allowing FRET, immunoassays (see sections 4.1 and 4.2), or specific probes for enzyme substrates or reaction products.[139] In addition, the activity of some enzymes such as α-amylase, aqualysin I, exonuclease, or malic enzymes, may be modulated by lanthanide ions.[140] Alternatively, enzyme-amplified lanthanide luminescence reflects enzymatic activity which produces molecules forming highly luminescent complexes with lanthanides; examples are oxidation of salicylaldehyde to salicylic acid catalyzed by xanthene oxidase or the transformation of 1,10-phenanthroline-2,9-dicarboxylic acid dihydrazide into its dicarboxylic form by hydroxide peroxide produced by the oxidation of β-D-glucose in the presence of the enzyme glucose oxidase.[141] Following this concept, a method for assaying the substrate specificity of proteolytic enzymes, which comprise an estimated 2% of the human genome, has been proposed. Fluorogenic peptide libraries are synthesized to probe substrate specificity in the prime sites of proteolytic enzymes, and their utility is demonstrated for the determination of the extended prime site specificity of bovine α-chymotrypsin. The peptide chains are decorated with a fluorosalicylic group acting as antenna for Tb^{III} luminescence.[142] The technology has been applied to the determination of tyrosine phosphatase activity[143] and for identifying selective substrates for this enzyme as well as potential inhibitors.[144] Modulation of lanthanide luminescence by switching on or off photoinduced electron transfer has resulted in the synthesis of three-component probes featuring a lanthanide chelate, an antenna, and a luminescence switch.[145] On the basis of this principle, a general platform has been designed for ratiometric analysis, which features a mixture of Eu^{III} and Tb^{III}; the relative contribution of each ion to the luminescence spectrum is tuned by adjusting the stoichiometry of the mixture and the ratio of the luminescence intensities is sensitive to environmental changes experienced by the antenna. This system has been tested for the determination of esterase activity.[146]

When it comes to direct use of LLBs, analyses are generally conducted in such a way as to evidence either the consumption of substrates or the formation of products of enzymatic activity. Among these products, the most relevant are protons, oxygen, hydrogen peroxide, and phosphates (inorganic phosphate, pyrophosphate, adenosine triphosphate (ATP), adenosine diphosphate (ADP), cyclic adenosine monophosphate (cAMP), as well as their guanidyl analogues). Information on enzyme kinetics is also at reach with selective luminescent probes having fast response and therefore allowing "on-line" analysis.

Chart 5. (Top) Selected Cyclen Derivatives L17−L19 for pH- and pO_2-Sensitive Eu and Tb Complexes; (Bottom) Gallamide Used as Gelator

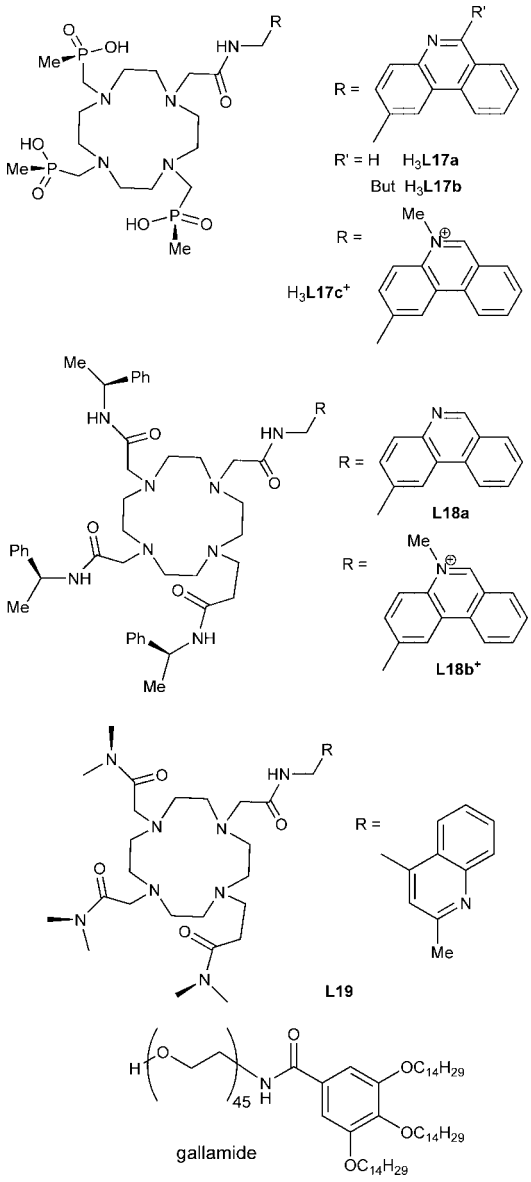

4.1.1. pH Probes

Protonation of basic sites in systems comprising a chromophore and a luminescent metal center often leads to cancellation of photoinduced electron transfer, opening the way to pH sensors. Some initially proposed systems were based on terpyridine derivatives but were not stable enough in water.[147] More robust sensors have subsequently been proposed,[105,148,149] in which the core is a substituted cyclen macrocycle usually bearing three phosphinate or carboxylate groups and a monoamide or four amide coordinating groups (Chart 5). A grafted phenanthridine moiety with a triplet state energy around 22000 cm^{-1} functions as light-harvesting unit able to sensitize efficiently the luminescence of Eu^{III} and, depending on the peculiar system, of Tb^{III}, although in this case the small energy gap between the triplet state and $Tb(^5D_4)$ may result in some back energy transfer. Protonation or alkylation of the sensitizer allows excitation wavelengths up to 370 nm, that is at the beginning of the visible range is a definitive asset if cheap instrumentation is to be designed. When excited at this wavelength, [Eu(**L17a**)], [Eu(**L17b**)], and [Eu(**L18a**)]$^{3+}$ display metal-centered emission which increases by about 6-fold when decreasing the pH of the solution from 6 to 2; analysis of the resulting S-shaped intensity-versus-pH curve yields excited state pK_as of 4.4, 4.35, and 3.3, respectively.[150]

Quinoline is also an adequate pH-responsive chromophore: both [Ln(**L19**)] chelates with Ln = Eu[151] and Tb[152] have pH-dependent emission in the range 5.5−7.5 and excited state pK_as were found to be 5.3 (quinoline amine) and 9.3 (quinoline amide) for [Tb(**L19**)]$^{3+}$.[153]

Soft materials such as hydrogels are permeable to water and provide unique and shielding environments for lanthanide luminescent sensors. For instance, doping $NH_4[Eu(tta)_4]$ into gallamide (Chart 5) results in a reversible on/off switching of the Eu-based luminescence in the pH range 3−4; in addition, both the thermal and photo stabilities of the tetrakis β-diketonate complex are improved with respect to aqueous solution.[154] Another optical pH sensor film for analysis of body fluids takes advantage of upconversion luminescence and has been produced from a mixture of $NaYF_4$:Er,Yb nanorods, the pH indicator bromothymol blue (BTB), and a biocompatible polyurethane hydrogel dissolved in ethanol. Deposition of the solution on a polyethylene terephthalate support and subsequent evaporation of the solvent yielded a $\approx 12\ \mu$m pH-responsive film. The effect of pH on the green and red emission of Er^{III} is due to the varying inner-filter effect of BTB with pH. Response in the pH range 6−10 is obtained in 30 s under NIR irradiation at 980 nm, a wavelength to which biological fluids and tissues are transparent.[155]

4.1.2. Oxygen and Singlet Oxygen Probes

There exists a wealth of luminescent oxygen sensors, some of them incorporated on ready-for-use microwell plates[139] and many based on lanthanide luminescence.[105,139,152,156−158] The rate of quenching of the triplet state in [Tb(**L17a**)], [Tb(**L18a**)]$^{3+}$, and [Tb(**L18b**)]$^{4+}$ by triplet oxygen, $k_q[O_2]$, is competitive with the rate of energy transfer onto the metal ion so that emission from these complexes is sensitive to the amount of dissolved oxygen; [Tb(**L17a**)] is also pH sensitive, giving [Tb(H**L17a**)]$^+$, while the *N*-methylated complexes are not and work well in the concentration range of 0−0.3 mM dissolved O_2.[159]

A miniaturized microelectronic sensor platform for atmospheric oxygen gas has been recently proposed, which could have interesting developments in biosensing. The highly conductive and spectroscopically transparent chemoresistor device is composed of single wall carbon nanotubes (SWNT) onto which dendrimer molecules containing eight Eu^{III} ions are immobilized (Eu_8SWNT). The device is activated by initial irradiation at 365 nm for populating electron taps on the substrate interface. It then shows linear sensitivity toward oxygen in the concentration range 5−27% and operates at room temperature and ambient pressure, features which are not shared by most solid state oxygen sensors.[156]

Singlet oxygen $^1O_2$ is a cytotoxic species oxidizing proteins, DNA, and lipids; it is involved in the cell signaling cascade, induces gene expression, and eventually leads to apoptosis, a property used in photodynamic treatment of cancer in which singlet oxygen is generated photodynamically in situ by energy transfer from a dye triplet state.[160−162] Such reactions also occur in cells containing chlorophyll, leading to photoinhibition of photosynthesis.[163] The weak and short-lived emission of singlet oxygen at 1.27 μm is

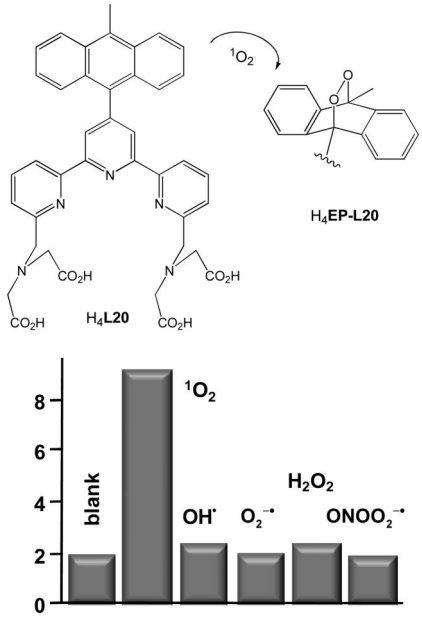

Figure 10. Singlet oxygen europium probe: formula of the ligand (top) and selectivity (bottom; vertical scale: luminescence intensity in arbitrary units) (redrawn from ref 164. Copyright American Chemical Society).

difficult to monitor directly under physiological conditions so that specific luminescent probes have been designed.[164−166] One of those is the highly stable europium complex [Eu(**L20**)]$^-$ (log $K \approx 21$), which specifically reacts with $^1O_2$ to yield its endoperoxide [Eu(**EP**−**L20**)]$^-$; the reaction is fast ($k \approx 10^{10}$ M^{-1} s^{-1}) and is accompanied by a sizable improvement in the photophysical properties: Q_L^{Eu} increases from 0.9 to 13.8% and $\tau(^5D_0)$ from 0.8 to 1.3 ms.[164] The selectivity of the probe system, which is insensitive to pH variation in the range 3−10, is adequate (Figure 10), with a limit of detection in water of 3.8 nM, about 20-fold lower than the highly sensitive chemiluminescent method of analysis based on tetrathiafulvalene derivatives.[167] HeLa (human cervical cancer) cells incubated simultaneously with [Eu(**L20**)$_3$]$^-$ and the sensitizer TMPyP (5,10,15,20-tetrakis(1-methyl-4-pyridinio)-porphyrin tetra-*p*-toluenesulfonate) take up both substances by endocytosis. Subsequent illumination at 450−490 nm followed by TR detection of Eu-centered luminescence (delay 0.4 ms) evidence the formation of singlet oxygen in the cells consecutive to the irradiation of TMPyP: as $^1O_2$ evolves, the intensity of the lanthanide emission increases, the luminescence intensity is smaller in the cytoplasm compared to the nucleus in which TMPyP localizes preferentially.[164]

4.2.3. Hydrogen Peroxide Probes

Hydrogen peroxide is produced by the activity of oxidases, which enables to assay the activity of the corresponding enzyme or of substrates such as glucose. Additionally, if an oxidase is used as a label, enzyme-linked immunoassays (ELISA) may rely on the detection of H_2O_2. Hydrogen peroxide can be detected with high sensitivity by chemiluminescence or electroluminescence, however, only at relatively high pH values. A lanthanide-based analytical procedure was proposed in 2002 by Wolfbeis and collaborators based on the finding that the europium complex with tetracycline (H_2**L21a**, Chart 6) binds H_2O_2, forming a luminescent ternary complex with a quantum yield of 4% at pH 6.9, representing a 15-fold increase with respect to the

Chart 6. Ligands for Hydrogen Peroxide and Phosphate Sensors

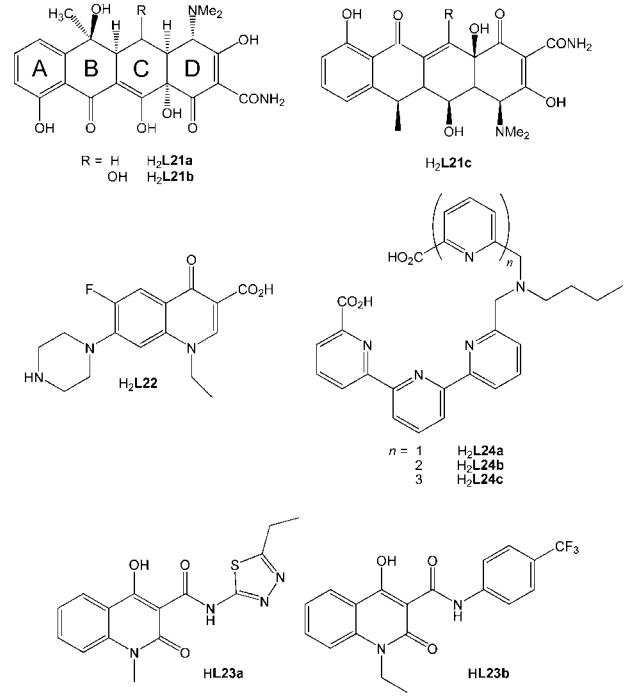

europium−tetracycline complex.[168] Tetracyclines are natural fermentation products of a soil bacterium, which act as antibiotics. In Chart 6, only the basic structure is shown, but substitutions at rings B through D result in an entire family of compounds. The stoichiometry of europium complexes with tetracyclines is not well established and depends on the substituents: 1:1, 2:3, and 3:2 Eu^{III}:L ratios have been reported. In the case of the parent ligand H_2**L21a**, the accepted stoichiometry is the one leading to the neutral species [Eu_2(**L21a**)$_3$] because tetracycline has two ionizable protons.[169] In the H_2O_2 probe system, however, a 3:1 stoichiometric ratio was used. Addition of enzyme to catalyze the reaction and of surfactant to enhance the luminescence intensity is not necessary and the reaction is complete in 10 min. The probe is excited at 405 nm by a diode laser and is effective in the range 2−400 μM (limit of detection, LOD = 1.8 μM, linear range 2−200 μM).[168]

Urea hydrogen peroxide can be assayed in the same way in human whole blood, providing a noninvasive method of analysis for the diagnosis of renal and cardiovascular diseases.[170] Several tests of enzyme activity (e.g., catalase) also rely on the europium−tetracycline probe allied with time-resolved detection; they have been developed so that standard microtiter plates associated with existing plate readers can be used. These assays are summarized in a recent review article.[171]

4.2.4. Phosphate Probes

A wealth of metal-based (M = Al, Zn, Cu, Cd) luminescent probes for phosphate derivatives, which operate at physiological pH and room temperature in aqueous solutions, are known. However, many of them require UV excitation, have low specificity, or do not work in presence of ubiquitous metal ions such as Ca^{II} or Mg^{II}.[139] Europium tetracycline probes used in TR mode perform better, with excitation wavelengths at 400 nm for the 1:1 complex with tetracycline H_2**L21a**[172] and 385 nm for the complexes with oxytetracy-

cline H_2**L21b**[173] and doxycycline H_2**L21c**[174] (Chart 6). Applied to the detection of adenosine triphosphate (ATP), which quenches the metal-centered luminescence, [Eu(**L21a**)]$^+$ proved to be less sensitive than the two other complexes, with LOD = 1.5 μM versus 2.7 and 0.4 nM for [Eu(**L21b**)]$^+$ and [Eu(**L21c**)]$^+$, respectively. The stoichiometry of the complexes with oxytetracycline and doxycycline is not given, but because the authors use solutions with a ratio Eu:L slightly smaller than 2, one may infer that it is probably 1:1 as well. On the other hand, the linear range of the assays with [Eu(**L21a**)]$^+$ is much larger: 0−25 μM as compared to 0.08−1.5 μM for [Eu(**L21b**)]$^+$ and 0.1−2.0 μM for [Eu(**L21c**)]$^+$. Finally, the probe can detect adenosine monophosphate (AMP, LOD = 2.5 μM), guanosine triphosphate (GTP, 1.8 μM), and pyrophosphates (PP, 1.0 μM) with about the same sensitivity. Moreover, adenosine diphosphate (ADP, 250 μM) generates little interference so that [Eu(**L21a**)]$^+$ has been applied to the detection of creatine kinase (CK) activity:

$$\text{creatine phosphate} + \text{ADP} \xrightarrow{\text{CK}} \text{creatine} + \text{ATP} \quad (19)$$

The one-step assay represents a welcome improvement over the standard two-step spectrophotometric assay and works in the range 0.05−2.0 units per milliliter (U mL^{-1}), which covers the range exhibited by cardiac infarction patients (0.08−0.6 U mL^{-1}).[172] Emission from the terbium complex with norfloxacin (Tb:H_2**L22** ratio 4.5:1) exhibits a 5-fold increase upon interaction with ATP and has also been proposed as probe of this analyte. Earlier work on ATP analysis was based on the [Eu(tta)$_3$] diketonate inserted into nonionic polyoxy-ethyleneglycol dodecyl ether (Brij-35) micelles; the reported limit of detection is 0.6 μM (linear range 1−100 μM), a value which can be lowered by about 1 order of magnitude by adding Gd^{III}, which generates columinescence. In this way, ATP could be determined in fruit juices with a limit of detection of 0.08 μM. However, the choice of the chelate implies UV excitation (330 nm).[175]

Ionic phosphate is a crucial nutrient and essential in metabolism, and several optical, electrochemical, and enzymatic methods of analysis have been proposed for its determination in a wealth of samples, including plants, crops, and clinical samples. To meet the needs of high-throughput technology for clinical assays, the Eu^{III} complex with tetracycline H_2**L21a** was tested as a probe of ionic phosphate. The behavior of this system is complex, and emission intensity depends on both the pH and the Eu:L ratio. When a 1:1 ratio is used, ionic phosphate can be detected with LOD = 5 μM and a dynamic range 5−750 μM.[176] With a larger Eu:L ratio, the situation is different, as demonstrated by the assessment of the activity of alkaline phosphatase (ALP) in a single-step end-point method taking advantage of the luminescence enhancement of the bioprobe in presence of phosphate; the stoichiometry used for these assays is 3:1. In presence of phosphate, this anion is produced when added phenyl phosphate is enzymatically hydrolyzed by ALP, the limit of detection of which reaches 4 μM.[177] Another procedure for the determination of ALP in drug tablets relies on luminescence quenching of [Tb(**L23a,b**]$^{2+}$ complexes by phosphate ions. The assay is conducted with equimolar concentrations of the ligand and Tb^{III} ions at pH 8 and leads to a much lower limit of detection: 40 pM, or 0.05 mU mL^{-1} (linear range 0.1−70 mU mL^{-1}). Ligand H_2**L23a** is used for the ALP assay, while H_2**L23b** performs well for the determination of codeine phosphate in the same samples, with LOD = 120 μg mL^{-1} (linear range 0.3−20 μg mL^{-1}).[178] More recently, the series of ligands H_2**L24a−c** was tested and the complex [Eu(**L24b**)$(H_2O)_2$]$^+$ was found to significantly interact with ATP at pH 7, positioning this system as a potential ATP probe.[179]

4.2.5. Enzyme Kinetics

Guanine nucleotide binding proteins consist of several subunits, one of which comprises those of the so-called rat sarcoma (Ras) family. These proteins are essential components of the signal transduction pathway and thereby control cell growth, differentiation, and apoptosis. Ras GTPases act as binary switches by converting guadenosine triphosphate (GTP) into guadenosine diphosphate (GDP). Luminescence of the Tb^{III} complex with norfloxacin (H_2**L22**, stoichiometric ratio used 4.5:1 Tb:L) is sensitive to the concentration of phosphate released by the GTP to GDP transformation, because the ion induces quenching. In vitro and real-time monitoring of GTPase activity is thus possible, and a microwell plate assay has been optimized for this detection in wild-type Ras and Ras mutants, avoiding using fluorescent-labeled GTP substrates which interfere with enzymatic activity.[180]

4.5. DNA Analysis

Most molecular biological and diagnostic applications require accurate quantification of nucleic acids extracted from various sources (e.g., blood, cells, bones). The simplest method for the determination of DNA is based on its ultraviolet absorption band at 260 nm, with an estimated molar absorption coefficient of 50 $\mu g^{-1} \cdot cm^{-1} \cdot mL$.[181] This method, however, bears several flaws. First, the molar absorption coefficient may slightly vary from one source of DNA to the other. Second, large sample volumes are needed. Third, the dynamic range is narrow and the method is sensitive to pH and salt content. Finally, contributions to the 260 nm absorbance by contaminating agents such as proteins and free nucleotides often lead to an overestimation of the DNA concentration. Thus fluorometric DNA assays have been developed using intercalating fluorescent reagents which display enhanced fluorescence intensity when interacting with DNA;[2,182] examples are ethidium bromide (EB),[183] the bis(benzimidazole) dye Hoechst 33258,[184] and the cyanine dyes PicoGreen[185] and SYBR Green I.[186−188] Some of these dyes have their own disadvantages. For instance, EB has a high intrinsic fluorescence which limits the sensitivity of the assays and it binds both RNA and ssDNA. In the presence of single-stranded nucleic acids, Hoechst 33258 stain is only selective for dsDNA if high salt concentrations are used; on the other hand, low salt concentrations allow the detection of both dsDNA and ssDNA/RNA.[184] Furthermore, this dye preferentially associates with A-T rich domains in DNA[189] and shows a reduced binding for DNA fragments <500 bp,[190] which may result in underestimating the DNA content. The dsDNA binding dyes PicoGreen (linear range 0.25−1000 pg μL^{-1} DNA)[185] and SYBR Green I (0.25−2500 pg μL^{-1})[188] have similar characteristics; they are not affected by a variety of contaminants but they are highly sensitive to photobleaching so that they should be used immediately after preparation of their solutions. The specificity of the fluorescence DNA

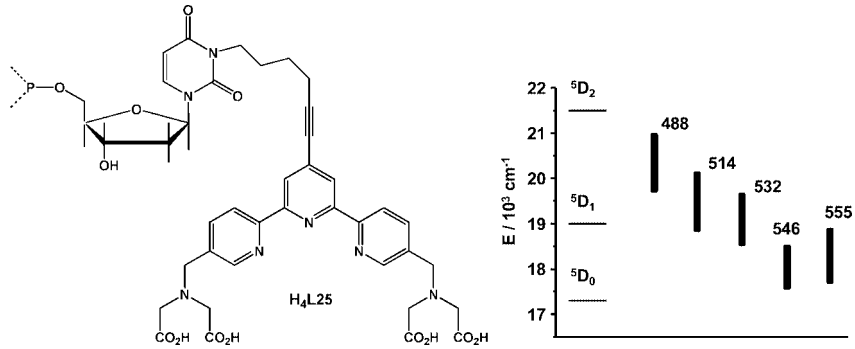

Figure 11. (Left) Structure of the phosphoramidite ligand for nFRET assays. (Right) Comparison between Eu^{III}excited state energies and the absorption energies (half-width is shown) of various Alexa dyes. (Redrawn from ref 199. Copyright American Chemical Society.)

analyses can be enhanced by bis-intercalating dyes such as thiazo (TOTO-3) or ethidium dimers (EtD),[191,192] which have association constants with DNA 10^3 times larger than monointercalators, almost no autofluorescence in water, and with which linear responses have been obtained in the 0.5−100 pg μL^{-1} range.[193] Methods using FRET have good sensitivity and are also widely used in PCR-type analysis with technologies such as TaqMan,[194] Molecular Beacon,[195] or Scorpion.[196]

In parallel to these efforts, numerous protocols taking advantage of the specificity of the LLBs have been proposed because they enable integrated multianalyte detection.[197,198] The initial methods required enzymatic and/or hybridization reactions and were not optimum. Improvement came with the introduction of homogeneous assays based on nonoverlapping resonance energy transfer, nFRET.[199] In these analyses, the lanthanide probe, e.g., a europium chelate such as the phosphoramidite $[Eu(\mathbf{L25})]^-$ (Figure 11) attached to the 3′ end of a 3′-TAC TTA TAT CTA TGT CTTC-5′ sequence transfers energy onto Alexa Fluor dyes conjugated to an amino-modified 3′-AAA TTA TAG TAA CCA CAAA-5′ sequence. Here the underlined letters denote bases which are noncomplementary to the target sequence and which prevent the probe of acting as primer during PCR. Changes in the lifetime of the acceptor upon hybridization with the target sequence dF508 of cystic fibrosis, 5′-TTA AAG AAAATA TCA TTG GTG TTT CCT ATG ATG AAT ATA GAT ACA GAA GCG TCA-3′, make direct separation of the hybridized and nonhybridized probes feasible by time-resolved detection. The limit of detection for the DNA target shown above is as low as 0.8 pM. The decay time of the organic fluorescent probe can be adjusted by changing the acceptor dye, which allows one-step multiplex homogeneous assays. It is noteworthy that the emission wavelengths of the organic dyes are shorter than the $Eu(^5D_0)$ emission, so that energy transfer occurs from upper excited levels of Eu^{III}. This is illustrated on the right part of Figure 11 in which the energies of the $Eu(^5D_J)$ levels are compared to the excited singlet state energies of a series of Alexa Fluor dyes. An additional proof comes from lifetime measurements. Because the organic dyes are excited by long-lived Eu^{III} levels, their decay time should mirror the lifetime of the feeding levels.[200] Indeed, Alexa 488 and 514, which are energetically above $Eu(^5D_1)$, have single exponential decay corresponding to a short lifetime (≈0.6 μs), while the other three dyes, which are amenable to transfer from both $Eu(^5D_1)$ and $Eu(^5D_2)$, display two-exponential decays with lifetimes ≈0.6 μs and 30−60 μs, respectively, in line with the longer lifetime of $^5D_1$. The efficiency of the Eu-to-Alexa dye transfer lies between 80 and 88%.[199] An alternative way of performing the analysis is to decorate both ends of the probe nucleotide with the lanthanide tag and with the organic acceptor, e.g., in Eu-TTT CCG CCT GCC GC-Alexa Fluor 647 (DP647) or in Eu-AAT CAG ACT GTT CAA GA-Alexa Fluor 700 (DP700; the underlined letters have the same meaning as above).

When unhybridized, the probe adopts a "random coil" conformation, which brings the donor and the acceptor in close proximity, thus allowing for efficient FRET transfer; on the other hand, when the probe is hybridized, the rigid double-stranded DNA chain forces the donor and the acceptor apart (≈3.4 Å/base pair) and both the energy transfer efficiency and the lifetime of the acceptor change so that the acceptor emission can be easily separated from the fluorescence of the unhybridized probe by enforcing an adequate time delay. The longer the d−a distance is, the longer the lifetime of the acceptor. This one-step procedure has been extended to dual analyte detection. High sensitivity is reached, for instance for celiac-disease related single nucleotide polymorphisms DQB1*0302 (CTC GGC GGC AGG CGG CCCC, probe DP647) or DQA1*05 (CAT AAC TTG AAC AGT CTG ATT AAA CGC, probe DP670), with detection limits in the 150 pM range.[130]

A somewhat simpler, although very robust and easy to implement approach relies on the disappearance of the quenching of a Eu^{III} binuclear helicate by acridine orange upon interaction of the latter with DNA. This quantification method is versatile, pH independent, insensitive to the presence of potentially interfering substances, adaptable to several kinds of DNA as well as to PCR products having a small number of base pairs (typically < 500), and necessitates standard time-resolved equipment. The neutral, water-soluble $[Eu_2(\mathbf{L43b})_3]$ helicate (see Chart 12, section 5.4) is thermodynamically stable, kinetically inert, possess long $Eu(^5D_0)$ lifetimes, is highly luminescent ($Q^L_{Eu} = 21\%$), and resistant to photobleaching. Its emission intensity and lifetime are dramatically quenched by selective fluorescent stains for nucleic acids such as ethidium bromide and acridine orange (AO) but are restored in the presence of nucleic acids (Figure 12). The method has been tested with actin sense-2 (oligonucleotide, ssDNA), plasmid (circular dsDNA), λDNA/*Hind*III (dsDNA), and sheared salmon sperm (genomic, dsDNA) DNAs as well as with PCR products; it is insensitive to pH variations in the range 3−10 and to 100−1000 fold excess of potential interfering substances such as BSA, glucose, citrate, urate, ascorbate, and several divalent or trivalent cations (Ca^{II}, Zn^{II}, Fe^{II}, Fe^{III}); on the other hand, Mn^{II}, Cu^{II}, and Co^{II} have detrimental effects when added in these proportions. Limits of detection for the four types of DNAs mentioned above are in the range 0.2−1.1

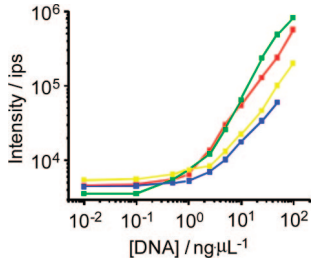

Figure 12. Intensity of the Eu^{III} luminescence measured in time-resolved mode upon addition of DNA to 0.1 μM [Eu_2(**L43b**)$_3$] + 33.1 μM AO in Tris-HCl buffer 0.1 M (pH 7.4). Key: actin sens-2 DNA, red curve; plasmid DNA, green curve; λDNA/*Hind*III, blue curve; salmon sperm DNA, yellow curve. (Redrawn from ref 74. Copyright Royal Society of Chemistry.)

Chart 7. (Top) Coumarin-Derivatized dtpa Ligand;[201] (Bottom) DTBTA Chelating Agent for Ligand-Based Assays of DNA Variation on Microarrays[203,204]

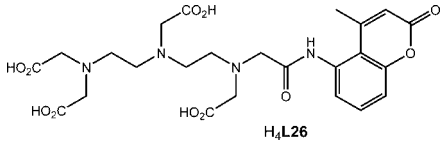

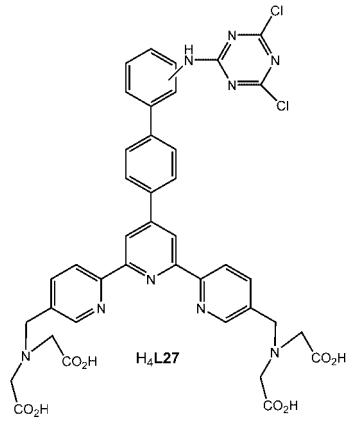

ng μL^{-1}, while PCR products such as a 347 bp fragment of β-actin gene can be detected with the same sensitivity as provided by the PicoGreen method.[74]

Introducing the LLBs into nanoparticles considerably enhances their sensitivity. As an example, silica nanoparticles ($d \approx 55$ nm) into which europium complexes with 7-amino-4-methylcoumarin derivatized dtpa, [Eu(**L26**)]$^-$ (Chart 7), have been introduced by reverse microemulsion technique display a luminescence intensity ≈1300-fold larger than the pure chelates. They have been bioconjugated to the biotinylated 5′-biotin-(T)10-TG CGG CAG GTG CGA CGC GGT-3′ nucleotide and a sandwich hybridization DNA assay based on magnetic microbeads as the solid phase carrier showed a detection limit of 160 pmol L^{-1} for the target DNA 3′-C GCC GTC CAC GCT GCG CCA CAG ATG GTC CGT AAG CGA-5′ under time-resolved detection.[201]

Single nucleotide polymorphisms (SNPs) are the most abundant form of DNA sequence variation in the human genome and are responsible for phenotypic diversity. They are used as markers in medical diagnosis, particularly with the aim of developing personalized medical treatments. Their large density, however, requires particularly powerful methods of analysis able to screen very large number of SNPs, and various approaches have been proposed based on hybridization of allele specific oligonucleotides (ASO) and combining analytical methods such as aggregation of nanoparticles, electrochemical and microarray sensing as well as FRET. Biochemical techniques have also been applied, e.g., enzymatic reactions such as allele specific PCR or DNA primer extension.[100] All these methods are multistep procedures and some require sophisticated instrumentation or are limited by experimental factors such as temperature, pH, or ionic strength. Most of these drawbacks can be overcome with LLBs, and Kitamura et al. have engineered a highly sensitive "colorimetric" analysis similar to homogeneous immunoassays in its principle. It involves DNA-templated cooperative complexation between a lanthanide luminescent ion (Eu^{III} or Tb^{III}) and two oligodeoxyribonucleotide conjugates, one fitted with a polyaminocarboxylate (edta, dtpa) as chelating unit and the other decorated with an aromatic polyamine (1,10-phenanthroline, terpyridine, or dipyrido[3,2-*a*:2′,3′-*c*]phenazine, dppz) as sensitizing chromophore.[100,205,206] The conjugates form a tandem duplex with the target in such a way that the auxiliary units face each other and build a coordinative environment for the Ln^{III} ions. Two situations are described in Figure 13: the Ln^{III} conjugate with the C base recognizes the wild type (WT) gene while the conjugate with the G base is specific for a mutant gene (mut). A proof-of-concept has been provided for the recognition of the thiopurine *S*-methyltransferase gene. By adding two allele specific recognition solutions, one containing Eu^{III} (mut recognition) and the other Tb^{III} (WT recognition), to target solutions of 27 mer sequences of the wild type gene, the mutant gene, or a mixture of both, green, red, and yellow colors are obtained under time-gated detection.[206] The target solutions correspond to possible genotype, homozygous wild type, homozygous mutant, or heterozygote, respectively. It is noteworthy that only the combination of edta and 1,10-phenanthroline provides sufficient emission in the presence of the targets. The quantum yields are modest, 1.5% and 3.3% for the Eu^{III} and Tb^{III} conjugates, respectively,[100] and a design of the coordinative cavity better preventing non-radiative deactivations would certainly improve considerably the sensitivity of the assays.

Discrimination of single-nucleotide mutations responsible for diseases with a large number of possible variations, such as cystic fibrosis for which more than 800 mutant variations are known, requires high-throughput devices, and DNA microarrays are useful tools in this respect. When variations of many genes or variations at different positions in a target gene must be detected in parallel at the same time on a microarray, simple hybridization-based assays are not sufficient. In addition, it is difficult to design several hybridization probes with nearly the same performance for distinguishing one-base variation under the same hybridization conditions. This can be overcome with ligand-based assays on microarrays based on the luminescence of a lanthanide chelate, namely [Eu(**L27**)]$^-$ (Chart 7). The latter is conjugated to avidin and the immobilized nucleotide sequence is detected by time-resolved luminescence following the specific coupling between avidin and the biotinylated probes 5′-P-GGC GCC CAC CAC CAG CT-biotin-3′ (recognized by glycine-type probes) or 5′-P-CGG CGC CCA CCA CCA GCT-biotin-3′ (recognized by valine-type probes) which specifically couple with the Eu-avidin conjugate. The technology has been successfully applied to genomic DNAs isolated from human umbilical vein endothelial cells (HUVEC) and human urinary bladder carcinoma T24 cells.[203]

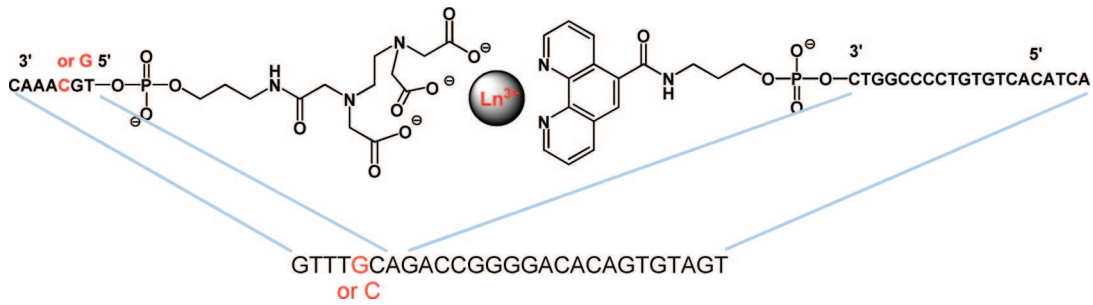

Figure 13. Example of a DNA-templated lanthanide luminescent bioprobe and its target (wild-type or mutant of the thiopurine *S*-methyltransferase gene). (Redrawn from ref 206. Copyright Oxford University Press.)

Chart 8. Cyclen Derivatives for *ss*-DNA and Analyte Sensing

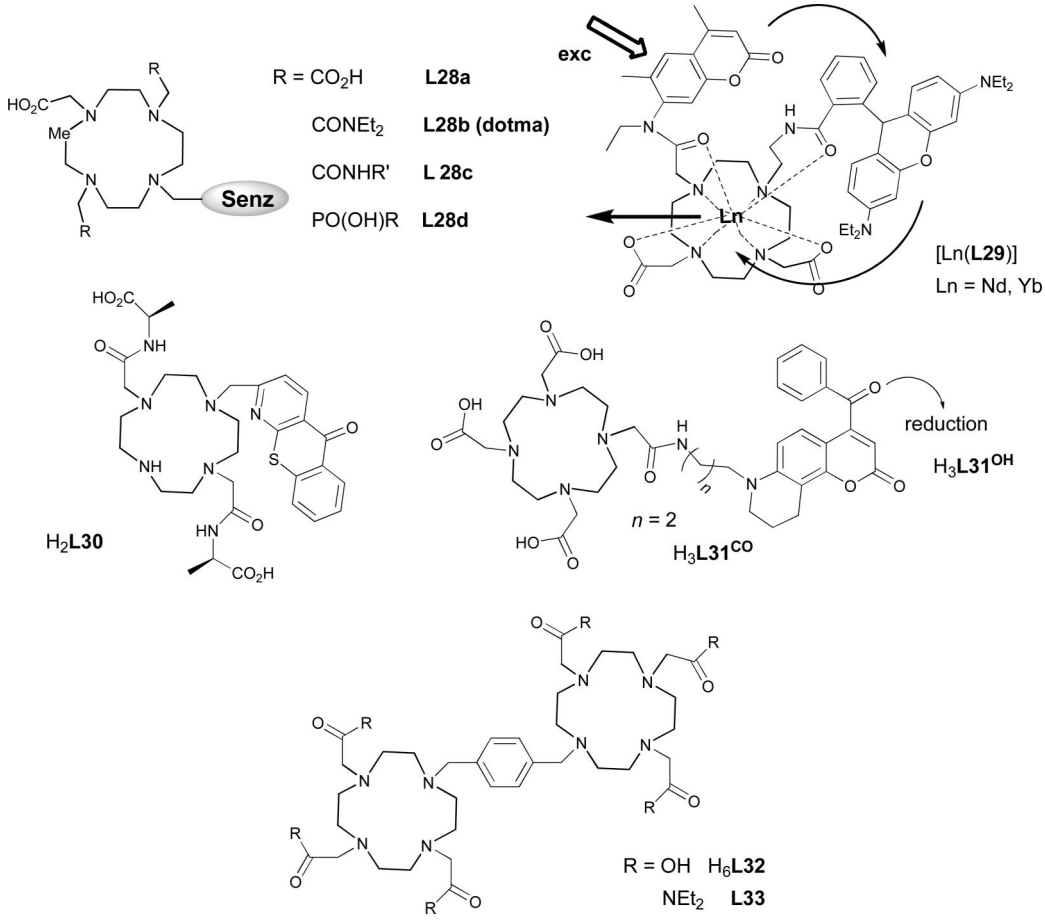

Among the wealth of LLB-based protocols for DNA analysis, recent papers describe the use of inorganic-hybrid materials,[207] quantitative analysis of genetic mutations caused by polycystic kidney disease with magnetic and luminescent nanoparticles,[208] or the sensitive identification of DNA quadruplexes in guanine-rich telomers located at the end of the eukaryotic chromosome with the help of Eu^{III} luminescence.[209] Luminescent heterometallic 5d−4f probes emitting both in the visible and near-infrared have been shown to be adequate reporters of the interaction of the binuclear chelates with *ss*-DNA. A $[Ru(tpy)_3]^{2+}$ unit, covalently linked to an Yb^{III} complex with a dotma derivative $[Yb(\mathbf{L28b})]^{5+}$ (see Chart 8; Senz = $[Ru(tpy)_3]^{2+}$). In the absence of interaction with DNA, the Ru^{II} moiety acts as sensitizer and MLCT-to-$Yb(^2F_{5/2})$ partly occurs, therefore upon excitation in the charge transfer band (448 nm), emission is seen from both Ru^{II} (605 nm) and Yb^{III} (978 nm). The latter signal is switched off upon binding to *ss*-DNA.[210] The cyclen complexes [Ln(**L29**)] (Ln = Nd, Yb) also act as NIR DNA probes: the cascade energy transfers which populate the metal-ion excited states is interrupted when the coumarin moiety interacts with *ds*-DNA.[211]

4.6. Detection and Quantification of Simple Analytes

A series of successful lanthanide responsive probes for quantifying analytes of biological relevance are based on the cyclen framework (Chart 8).[16,106,212−214] The latter usually features three coordinating units (carboxylates, substituted amides, phosphinates) and one sensitizing pendant, which often simultaneously binds the central metal ion. Signaling is achieved by enhancing or quenching the metal-centered luminescence, the latter often through a photoinduced electron transfer.[215] Typical analytes which can be quantified are pH,[216] $p(O_2)$, various simple anions (halides, nitrate,

HPO_4^{2-}, SO_4^{2-}, acetate, oxalate, malonate, succinate, lactate, citrate),[217−219] β-diketonates,[220] or amino acids.[213,221] One of the most remarkable results reported recently is a nonenzymatic, ratiometric method for the selective determination of lactate and citrate in microliter samples of human serum, urine, or prostate fluids for diagnosis of prostate cancer. These two anions are crucial entities in the metabolism of the cells, with lactate being the end product of anaerobic and hypoxic glucose metabolism, while citrate is a key intermediate in the Krebs cycle of aerobic cells. Both analytes are important in diagnosis, for instance, lactate concentration is higher than normal in liver diseases. Reduced levels of citrate in urine are diagnostic of various kidney dysfunctions and of malignant prostate cancer in which they are reduced from the normal 10−12 to 1−3 μmol g^{-1}. Binding of citrate onto $[Eu(H_2O)(\mathbf{L30})]^+$ (log $K = 4.5$) results in an increase in Eu($^5D_0$) lifetime and in a change in the intensity ratio of the transitions to $^7F_2$ and $^7F_1$. Analysis of 17 samples of prostate fluid by the luminescent ratiometric method and by a commercially available citrate lyase enzyme kit gave the same results in the range 12−160 mM. The luminescence method is much faster and requires about 25 times less biofluid (1 μL).[222]

Cyclen complexes also act as luminescent reporter substrates for redox metabolism; for instance, $[Nd(\mathbf{L31^{CO}})]$ sees its metal-centered NIR luminescence switched on upon reduction of the ketone group into alcohol, leading to $[Nd(\mathbf{L31^{OH}})]$; such sensors are able to detect human aldo-keto-reductases which are involved in steroid hormone metabolism and stress response mechanisms.[223] To increase the efficiency of cyclen-based LLBs, bis(cyclen) receptors have been designed in which the two coordinative macrocycles are linked, for instance, by a xylene group (H_6**L32**, **L33**, Chart 8), which can act as a sensitizer chromophore; in this way, two monodentate ions can be detected simultaneously or, alternatively, a single bidentate anion.[12,224]

Alternate substrates to cyclen derivatives have been used for similar purposes, for instance chiral tripodal ligands for the analysis of anions,[225,226] dendrimeric complexes for NIR detection of anions,[227] polyaminocarboxylates immobilized on sensory chips for detection and separation of histidine-tagged ubiquitin proteins,[228] or transferrin and lactoferrin complexes of Tb^{III} for pH sensing.[229]

5. Cell and Tissue Imaging

As the usefulness of LLBs unfolded its promising properties in bioanalyses, attempts to apply them for imaging purposes were a natural follow up. Given that many lanthanide complexes are cell-permeable and that techniques of time-resolved detection in microscopy are well mastered,[9,230] scientists have used the unique spectroscopic properties of Ln^{III} ions to obtain images of cells, for instance in the context of the follow up of cancer therapy. LLBs are also able to signal the presence of many important analytes (e.g., Ca^{II}, bicarbonate, ascorbate, urate) the fluctuations of which are tractable with high spatial resolution and yield information of utmost importance on cellular metabolism. Optical probes are unique for this task because acquisition of signals is fast. Specific modification of the LLBs, or their bioconjugation, furthermore opens the door to deciphering where analytes accumulate in live cells and what their concentrations are in the various cell organelles.

Chart 9. Formulae of the Some Chelating Agents Used in Initial Time-Resolved Microscopy Experiments

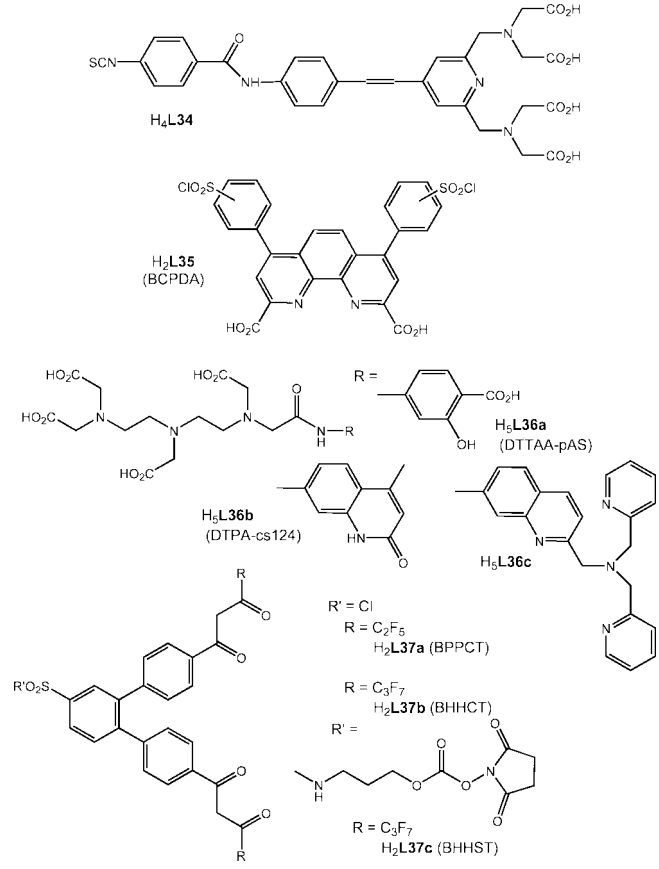

5.1. Microscope Design and Initial Experiments

Initial experiments dealing with cell imaging with the help of lanthanide chelates described (i) the staining of bacterial smears from *E. coli* cell walls,[4] (ii) the localization of rabbit immunoglobulin G (IgG) into a histological section of human smooth muscle myosin with an Eu^{III} polyaminocarboxylate ($[Eu(\mathbf{L34})]^-$, code W1014,[231] Chart 9) conjugate with swine antirabbit IgG,[232] (iii) the detection of malignant tumors in C-57 dark-fur mice with the help of Yb^{III} NIR-emission,[233] and (iv) how the nature of the binding sites on the cell walls of *Datura innoxia* can be elucidated by addition of Eu^{III} chloride[234] but no advantage was taken from time-gated detection in these early works. However, it was soon realized that such a detection will considerably improve the quality of the images,[9] and the first report describing the design of a time-resolved microscope used in conjunction with an Eu^{III} probe dates back to 1990:[235] an epi-fluorescence microscope equipped with a xenon flash lamp was modified by addition of a chopper the velocity of which was chosen to generate a 250 μs delay. Eu^{III}-doped yttrium oxysulfide nanoparticles were milled to an average size of 100−300 nm in the presence of polycarboxylic acid to avoid aggregation and subsequently conjugated to avidin and other proteins such as protein A or IgG by simple adsorption on their surface. These conjugates performed well as time-resolved LLBs, as demonstrated by immunocytochemical reactions on latex beads and microscopy imaging with a CCD camera. A very similar instrumental setup was proposed by Seveus et al.[236] The Eu−W1014 complex, which suffered from some photostability problems, was replaced by the Eu^{III}−BCPDA (Chart 9) chelate conjugated to streptavidin or antisera. These Eu^{III} bioprobes allowed the detection of tumor-associated

antigen C242 in the malignant mucosa of human colon, of type II collagen mRNA in developing human cartilaginary growth plates, as well as of human papillomavirus 11 (HPV-11) specific gene sequences in the squamous epithelium of human cervix; immunohistochemical reactions were conducted on formaldehyde-fixed, wax-embedded tissue sections. The TR Eu-probe performed particularly well when cells were stabilized after the immunocytochemical reaction by glutaraldehyde fixation: the resulting strong autofluorescence is completely avoided and recorded signal-to-noise ratios were up to 2400:1.[237]

The xenon flash lamp can also be replaced by a continuous mercury or xenon arc lamp fitted with a chopper[238] and streptavidin cross-linked to thyroglobulin and multiply labeled with Eu-BCPDA (SBMC, streptavidin-based macromolecular complex) made possible time-resolution of double-emission images of living amoebae cells containing both lucifer yellow in pinocytosed vesicles and surface-bound SBMC-labeled biotinylated concanavalin.[239] But synchronizing two choppers may prove inconvenient, and attempts have been made to replace the detection chopper by a ferro-electric liquid crystal shutter.[240,241] Swiss albino mouse 3T3 cells stained with a Tb^{III} chelate, $[Tb(\mathbf{L36a})]^{2-}$ (Chart 9)[242] or with its conjugate with a lipid[243] have been imaged with such an experimental setup and their morphology determined.[241] The ferro-electric shutter results in an easier tuning of the time delay, unfortunately to the cost of a much reduced intensity (85% loss), so that most of the later designs used microchannel plate image intensifier coupled to a CCD detector. Amplification gains up to 10000 are obtained, and the detector can be gated with nanosecond resolution.[9] A combination of spectral and temporal resolution can be easily achieved with such a setup and with $[Eu(\mathbf{L36b})]^{2-}$.[244]

5.2. Further Developments

With TR microscopy at hand, immunocytochemical detections became quite sensitive and a wealth of analyses have been proposed, some of them are described here. The detection sensitivity of the earlier LLBs was hampered by their relatively low quantum yield. This can be overcome in cellular and tissue applications by tyramide signal amplification (TSA technology or CARD−catalyzed reporter deposition) via an enzyme-mediated method taking advantage of the catalytic activity of horseradish peroxidase to generate high-density labeling of a target protein or nucleic acid sequence in situ. In this way, immunocytochemical detection of vimentin in cryosections of rat liver can be achieved and the luminescence signal is strong enough to be seen by the naked eyes.[245] In other cases, such an amplification is not necessary, for instance, for the TR detection of circulating islet cell antibodies in insulin-dependent diabetes patients.[246,247] The Eu−BHHCT complex (Chart 9) has been bioconjugated to oligochitosan, which binds specifically to the membrane of tobacco cells; a sensitive assay has been developed for assessing the decrease in peroxidase produced in these cells and the increase in the concentration of indole-3-acetic acid both consecutive to the interaction with oligochitosan.[248] In another assay, addition of an Eu^{III} aryl-β diketonate to vessel specimens of an arteriovenous malformation swine model embolized with a mixture of *n*-butyl-2-cyanoacrylate and oil led to their easy differentiation.[249] Multiparameter imaging is also feasible, as demonstrated by A. E. Soini et al., who used a combination of four different metal luminophores (Eu^{III}, Tb^{III} chelates, and Pd^{II}, Pt^{II} coproporphyrins) in conjunction with an organic marker (Syto 25) to image samples containing mixed populations of peripheral blood leukocytes; emission from the various luminescent stains was separated by time-resolved detection.[250] Ligands bearing bipyridyl carboxylates units function as efficient antennae for several lanthanide ions and the Tb^{III} bioconjugate with BSA yielded highly contrasted time-resolved luminescence images of rat brain slices.[90]

Chart 10. Trimethoprim-Based Ligand for Designing Tb^{III} Conjugates

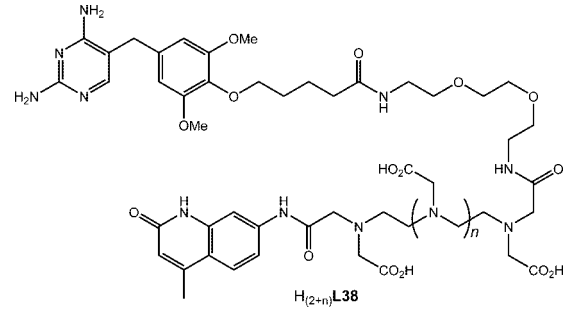

$H_{(2+n)}$**L38**

Tb^{III} complexes with bifunctional ligands containing trimethoprim as protein-binding unit and a polyaminocarboxylate moiety functionalized with carbostyril 124 for luminescence sensitization (Chart 10) have large quantum yield in water (30−40%) and bind strongly to *E. coli* dihydrofolate reductase (eDHFR) fusion proteins in vitro ($K_{as} \approx 10^9\ M^{-1}$). Time-resolved, luminescence microscopy with fast image acquisition then evidence the specific labeling of eDHFR expressed on the surface of living mammalian NIH3T3 fibroblast cells transfected with the corresponding plasmid DNA vector. On the other hand, when the cells were transfected with plasmid DNA expressing the nucleus-localized cyan fluorescent protein, no specific labeling of eDHFR was observed.[251]

Environmental samples of water contaminated with *Giardia lamblia* cysts, an intestinal parasite in human and animals causing diarrhea and which generates large autofluorescence signals, have been analyzed by TR microscopy with the help of the Eu^{III} chelate with BPPCT (Chart 9). A 60 μs delay resulted in a 30-fold increase in the signal-to-noise ratio.[252] A comparable improvement was later recorded on similar samples or on samples containing *Cryptosporidium* oocysts when the xenon flash lamp was replaced by an inexpensive light emitting diode and when the chelating agent was replaced by BHHST (Chart 9).[253]

5.3. Cyclen-Based Chelates as LLBs

Spatial and temporal variations of various analytes in live cells are vital information for the biochemist. In the course of an extensive and seminal investigation of over 60 different cyclen-based Eu^{III} and Tb^{III} LLBs fitted with various chromophores featuring tetraazatriphenylenes, acridones, azaxanthones, azathiaxanthones, or pyrazolyl azaxanthones[16,216,254−257] (see **L18a**, Chart 5; $\mathbf{H_2L30}$, Chart 8; **L39** and **L40**, Chart 11 for examples), Parker's group has established that the nature of the chromophore and its attachment mode to the macrocycle primarily determines the cell uptake and localization and not the charge of the complex or its lipophilicity. Quantum yields are on the order of 10% and 40% for Eu^{III} and Tb^{III} chelates, respectively. Among the cell lines studied were mouse skin fibroblasts (NIH-T3 cells), Chinese hamster ovarian (CHO), or cervical carcinoma HeLa cells. The reason

Chart 11. Examples of Cyclen-Based Ligands for Cell Imaging

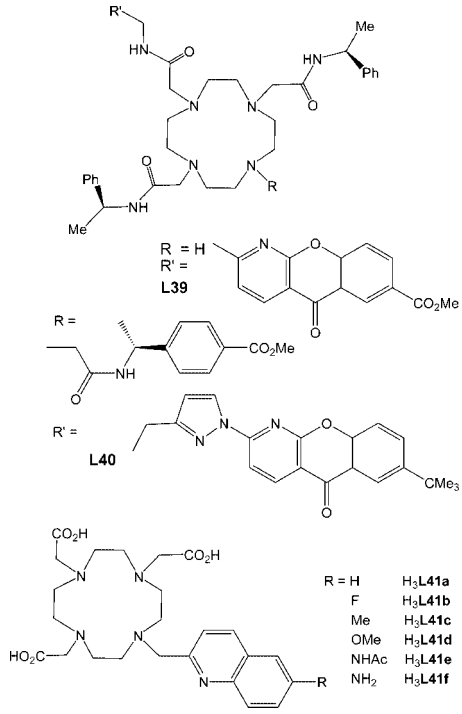

invoked is that polycyclic sensitizer units are recognized by protein association. Complexes staying in mitochondria have usually low IC_{50} values and cause cell apoptosis, while those internalized in lysosomes are nontoxic and therefore can act as responsive probes. About 80% of the macrocyclic complexes have endosomal/lysosomal localization; in these cases, the rates of uptake and egress are fast. Half a dozen of complexes also display fast uptake but slower egress and shuttle between mitochondria and endosomal/lysosomal compartments; [Eu(**L39**)]$^{3+}$ is such a chelate, with initial mitochondrial internalization (<4 h), final lysosomal localization (>14 h), and IC_{50} > 175 μM. On the other hand, [Eu(**L40**)]$^{3+}$ with IC_{50} = 58 μM stains both mitochondria and lysosomes and its localization is independent of time. Finally, a few complexes display slow uptake and egress and enter the ribosomes and the nucleoli. Their IC_{50} values are in the range 40−90 μM.[16] The nature of the substituent on the sensitizer unit of the macrocyclic ligand is a key factor with respect to the sensitivity of the LLB; it also strongly affects protein affinity.[258] The mechanism with which lanthanide cyclen chelates penetrate into live cells has also been investigated because it is critical to the development of imaging probes and therapeutic vectors. One of the major pathway is endocytosis (either clathrin- or caveolae-mediated) involving a vesicular uptake of the incoming chelate followed by invagination of the cell membrane. Other mechanisms are macropinocytosis and clathrin/caveolae-independent cytosis. Distinction between these mechanisms is made by monitoring the uptake in the presence of inhibitors/promoters of specific pathways. The dominant mechanism for cyclen Eu^{III} and Tb^{III} complexes seems to be macropinocytosis.[259]

Another, simpler series of cyclen derivatives are fitted with 6-derivatized quinoline moieties as sensitizers yielding neutral chelates [Eu(**L41**)] (Chart 11); the quantum yields are smaller than those exhibited by Parker's compounds (2.6−5.9%), but HeLa cells could be conveniently imaged.[260] In addition, emission from mixtures of [Eu(**L41d**−**e**)] (Chart 11) and [Tb(**L36b**)]$^{2-}$ (Chart 9) injected into the same cells can easily be spectrally separated by means of filters. The same authors also proposed Zn^{II} imaging in live HeLa cells with [Eu(**L36c**)]$^{2-}$ (Chart 9).

Chart 12. Ditopic, Hexadentate Ligands for the Self-Assembly of Binuclear Helicates

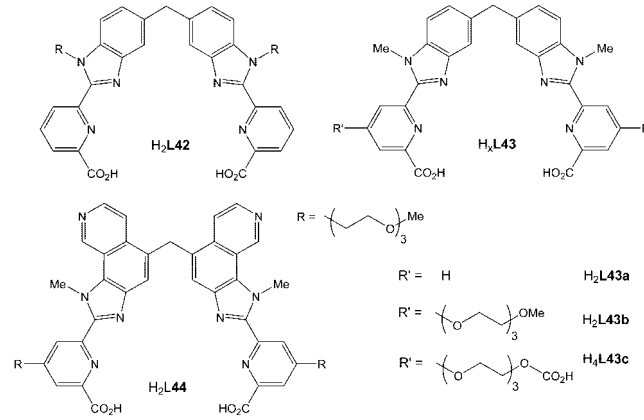

5.4. Binuclear Helicates as LLBs

Similarly to double lanthanide tags taking advantage of two lanthanide ions in one molecule,[261,262] another class of cell-imaging LLBs are binuclear helicates [Ln_2L_3] which self-assemble in water at pH 7.4 and room temperature.[263] The hexadentate ligands are derived from benzimidazolepyridine building blocks which act as adequate sensitizers of the luminescence of Ln^{III} ions. Polyoxyethylene pendants grafted either on the benzimidazole or pyridine aromatic moieties ensure water solubility and higher hydrophilicity of the helicates (Chart 12). The latter are thermodynamically stable and kinetically inert.[15,264] For instance, under stoichiometric conditions and at physiological pH, speciation diagrams for [Eu_2(**L43b**)$_3$] show that 98% of the metal ion is under the form of the binuclear helicate for a total ligand concentration of 10^{-4} M.[202] Several ligands have been tested,[202,265−268] and the best ones turned out to be (**L43b**)$^{2-}$, which sensitizes the luminescence of several lanthanides, primarily Eu^{III} (Q^L_{Ln} = 21%) and Tb^{III} (11%) but also Sm^{III} (0.4%) and Yb^{III} (0.15%), thus allowing multiplex analyses, as well as (**L44**)$^{2-}$ amenable to excitation at the beginning of the visible range. On the other hand, introducing a substituent on the benzimidazole ring had detrimental effect on the photophysical properties of the helicates.[266] All the chelates are noncytotoxic for HeLa (human cervix cancer), MCF-7 (human breast cancer), Jurkat (human T leukemia), 5D10 (mouse hybridoma), and HaCat (nonmalignant epithelial human cells) cell lines, with IC_{50} > 500 μM. The uptake in the cells is slow and proceeds by endocytosis, with a localization in the endoplasmatic reticulum (Figure 14), irrespective of the substituent or nature of the ligand core, as demonstrated by

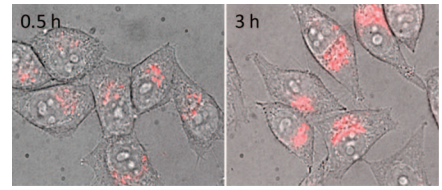

Figure 14. Merged bright-field and time-resolved luminescence microscopy of HeLa cells incubated 0.5 and 3 h with [Eu_2(**L43b**)$_3$] 200 μM and showing the localization in the endoplasmatic reticulum. (Adapted from ref 268. Copyright Wiley-VCH.)

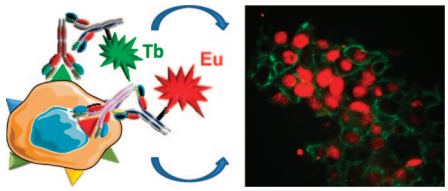

Figure 15. (Left) Principle of the lab-on-a-chip dual assay for estrogen receptors (nucleus) and human epidermal growth factor receptors (cell membrane) with binuclear Ln^{III} helicates $[Ln_2(\mathbf{L43c})_3]^{3-}$ conjugated to specific antibodies. (Right) Time-resolved microscopy of a breast cancer tissue section pressed into a 100 μm wide microchannel. (Redrawn from ref 274. Copyright Royal Society of Chemistry).

costaining experiments.[267,268] The average number of helicates per cell is in the range $2-5 \times 10^8$, much as that for the cyclen-based complexes.[255] Egress is also slow, and almost no leakage is seen after 24 h.[269] Similar properties are recorded when the polyoxyethylene chain is lengthened.[267]

The past few years have witnessed the advent of novel, more effective targeted therapies for cancer treatment. As a consequence, modern pathology laboratories are increasingly confronted with the need to reliably and efficiently identify relevant therapy targets on cancer tissues.[1] To respond to this demand, miniaturized bioanalytical systems are being developed[270,271] and applied for the detection of biomarkers in malignant tumors[272] and for the follow-up of patients with AIDS.[273] In this respect, LLBs combined with lab-on-a-chip microfluidics technology allow fast detection of these markers on sections of cancerous tissues. Our group has recently demonstrated the feasibility of this approach using a commercially available Eu^{3+} chelate.[14] The helicates $[Ln_2(\mathbf{L43c})_3]^{3-}$ (Ln = Eu, Tb) are amenable to coupling with proteins such as avidin or with antibodies and a simultaneous analysis of two biomarkers expressed by breast cancer cells, estrogen receptors (ER), and human epidermal growth factor receptors (Her2/*neu*) could be performed on tissue sections (Figure 15). The Ln helicates are coupled to two secondary antibodies: ER receptors are visualized by red-emitting Eu^{III} using goat antimouse IgG and Her2/*neu* receptors by green-emitting Tb^{III} using goat antirabbit IgG. The assay is more than 5 times faster and requires 5 times fewer reactants than conventional immunohistochemical assays which provides essential advantages over the latter for clinical biomarker detection.[274]

5.5. Overcoming Excitation Wavelength Limitation by Multiphoton Excitation

Most of the LLBs described above have to be excited around 350 nm, which is a somewhat short wavelength with respect to the integrity of the biological material. Shifting the excitation wavelength more toward the visible by modifying the ligand structure is feasible[104] but not always easy without substantial loss of emission intensity due to back transfer.[268] An alternative is to resort to two- or three-photon absorption, usually achieved with a femtosecond Ti:sapphire laser around 980 nm. Presently, luminescence microscopes with multiphoton excitation capability are commercially available[275] so that bioassays and imaging experiments taking advantage of long excitation wavelengths will develop substantially in the near future.[276] For instance, both cyclen-based[277,278] bioprobes and self-assembled binuclear helicates[279] are amenable to this type of excitation. Considerable work has also been done in designing suitable

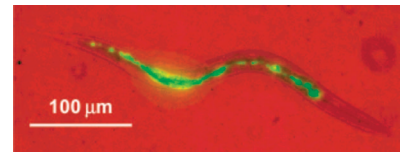

Figure 16. Two-photon image of *C. elegans* under 980 nm excitation. Emission from the up-converting phosphor Y_2O_3:Er^{III}(1%), Yb^{III}(2%) is shown in green. (Reproduced with permission from ref 288. Copyright American Chemical Society).

ligands and/or materials for this purpose which display large 2- and 3-photon absorption cross sections.[280] This is the case for instance of dipicolinic acid derivatives.[281−284] The use of multiphoton excitation in bioanalyses, bioimaging,[24,285,286] and photodynamic therapy of cancer[160] has been the subject of several recent reviews, so we do not discuss it further here.

5.6. Improving Sensitivity with Nanoparticles

As for immunoassays, the sensitivity of imaging experiments may be boosted by the use of nanoparticles and/or UCPs. Inorganic rare-earth containing up-converting nanophosphors exhibit unique imaging ability, as demonstrated by a new three-dimensional visualization method of laser scanning up-conversion luminescence microscopy based on a reverse excitation dichroic mirror and the confocal pinhole technique.[287]

The digestive system of the nematode worm *Caenorhabditis elegans* has been imaged by yttrium oxide nanoparticles (average size: 50−100 nm) doped with 1% Er^{III} and 2% Yb^{III}; they were prepared from thermal hydrolysis of the corresponding nitrates in the presence of urea and subsequently annealed at 1000 °C during 2 h. The phosphors are easily visible in the intestines, most nanoparticles being found beyond the pharynx and extending to the rectum (Figure 16). The phosphors are retained in the worms up to 24 h, when they are deprived of food because excretion is inhibited as feeding ceases. On the other hand, the bioprobes are excreted in 2 h if feeding is resumed.[288]

Up-converting $NaYbF_4$ microparticles doped with different Ln^{III} ions (Ln = Er^{III}, Tm^{III}, or Ho^{III}, or a combination of them) emit visible orange, yellow, green, cyan, blue, or pink light under NIR excitation. The emission color can be tuned by modifying either the dopant concentration or the dopant species. When the microparticles are surface-coated with silica, good dispersion in water in achieved; following amino functionalization, these microparticles (size $\approx$ 1.5 μm) were chemically conjugated with the rabbit anti-CEA8 antibody and then used as luminescent stains for the immune-labeling and imaging of HeLa cells.[134] Tissue imaging with up-conversion nanoparticles is also feasible, as demonstrated by the intravenous or intradermous injection of polyethyleneimine-coated $NaYF_4$:Er,Yb nanoparticles into rat tissues followed by 980 nm excitation.[96]

Deep tissue NIR-imaging (up to 1 cm) of the thigh and abdominal cavity of nude mice has been realized by injecting intramuscularly and intraperitoneally silica nanoparticles doped with neodymium fluoride. These nanoparticles have high quantum yield and can be excited at the beginning of the NIR range, at 730 nm, while the emitted light is observed at 1.06 μm (exposure time: 1 min). When the same nanoparticles were injected in the tail vein, the 1.06 μm signal could be seen from the ear lobe after 30 min and the time

frame of the experiment was fast enough (exposure time 0.1 s) to detect the particle flow in the body fluids.[289]

Nanorods of Eu^{III} hydroxide functionalized by a surface coating of phenoxybenzoate-containing silicate (ORMOSIL) as the sensitizer display intense red luminescence and are internalized in human lung carcinoma A 549 and HeLa cells; the nanorods localize in the cytoplasm, as seen under excitation at 400 nm (i.e., in the benzoate excited states) without cytotoxicity effect for at least 24 h.[290] Similarly, colloidal solutions of Eu^{III} hydroxide nanoparticles stabilized by polyvinyl alcohol or polyvinyl pyrolidone function as luminescent nanolabels for living sperm cells without inducing cytotoxicity.[291] Calcium ions in nanoparticles made of hydroxyapatite, which is a biocompatible, cell-penetrating material, can be easily replaced by Tb^{III} ions rendering them highly luminescent under direct 488 nm excitation. These particles have low toxicity and helped imaging mesenchymal stem cells from rabbit bone marrow.[292]

We also note that analysis of *Giardia lamblia* microorganisms has been attempted with nanoparticles containing a ternary Eu^{III} complex with BHHCT (H_2**L37b**, Chart 9) and 2-(*N,N*-diethylanilin-4-yl)-4,6-bis(3,5-dimethylpyrazol-1-yl)-1,3,5-triazine conjugated to 3-aminopropyl(triethoxy)silane. The quantum yield of the latter is large and the complex may be excited in the visible (up to 450 nm, maximum at 406 nm) allowing the use of cheap solid-state LED as excitation source.[293]

6. Perspectives

The examples of applications of LLBs described in the various sections of this review clearly point to the growing importance of lanthanide optical probes in all aspects of biosciences, from simple analyte quantitation to sophisticated imaging experiments on tissues and even live organisms. These probes benefit not only to medical diagnosis and therapy follow up but are more and more seen in many aspects of nanobiotechnology. One reason is that they ally high spatial resolution with easy time-gated discrimination and, when it comes to NIR-emitting probe, deep penetration depth.

Use of LLBs is relatively recent and despite the wealth of data accumulated during the past decade, there remains a lot to be learned. If ligand design to generate efficient sensitization of lanthanide luminescence is fairly well mastered on a trial-and-error basis, suitable modeling of the intricate energy transfer process has still to be improved. To benefit from the full advantage of NIR-emitting probes,[294] markers with better quantum yield and/or better emission intensity have to be tailored; a few examples already exist which rely on either inserting the luminescent stains into nanoparticles[289] or into large dendrimeric structures.[295] Moreover, if the use of sophisticated experimental techniques such as up-conversion, multiphoton excitation, time-resolved microscopy, or lab-on-a-chip devices is to be more spread out, better and cheaper instrumentation has to be developed. On a more biochemical level, the problematic of internalization of lanthanide chelates in given organelles of live cells is still half a mystery in that the relationship between structure and penetration/egress is not reliably established despite encouraging systematic efforts.[16]

Dual or multimodal probes bear a lot of promises. Evident examples are the simultaneous detection of two or several analytes[250,296] or of two biomarkers expressed by cancerous tissues.[14,297] Visible-emitting stains can also be combined with NIR-emitting ones.[210] When it comes to imaging, especially in vivo imaging, a combination of experimental techniques may help gaining improved and crucial information. Several systems have been proposed which combine MRI capability with optical lanthanides bioprobes;[210,261,298−303] in such dual assays, the optical probe may for instance serve to localize the MRI contrast agent or help visualize the delivery of nucleic acids into cultured cells.[304]

In conclusion, it appears that the door to the world of lanthanide luminescent bioprobes has only been slightly split open and that there is still plenty to harvest in this exciting new field of research which puts together disciplines such as analytical, coordination, and supramolecular chemistry, photophysics, nanotechnology, and medical diagnosis and therapy as well as biotechnology.

7. Acknowledgments

This work is supported by the Swiss National Science Foundation (grant 20020_119866) and by the Swiss Office for Science and Education within the frame of the COST Action D38 from the European Science Foundation (grant C07.0116). I am grateful to my present and past collaborators for their invaluable input, to Dr. Svetlana V. Eliseeva for a careful reading of the manuscript, and to the World Class University (WCU) Program from the Ministry of Education, Science and Technology, Republic of Korea (grant R31-10035).

8. References

(1) Glunde, K.; Jacobs, M. A.; Pathaka, A. P.; Artemov, D.; Bhujwalla, Z. M. *NMR Biomed.* **2009**, *22*, 92.
(2) Lakowicz, J. R. *Principles of Fluorescence Spectroscopy*, 3rd ed.; Springer Science: New York, 2006.
(3) Xing, Y.; Rao, J. *Cancer Biomed.* **2008**, *4*, 307.
(4) Scaff, W. L.; Dyer, D. L.; Mori, K. *J. Bacteriol.* **1969**, *98*, 246.
(5) Soini, E.; Hemmilä, I. *Clin. Chem.* **1979**, *25*, 353.
(6) Hemmilä, I.; Ståhlberg, T.; Mottram, P. *Bioanalytical Applications of Labelling Technologies*, 2nd ed.; Wallac Oy: Turku, Finland, 1995.
(7) Bazin, H.; Trinquet, E.; Mathis, G. *Rev. Mol. Biotechnol.* **2002**, *82*, 233.
(8) Hovinen, J.; Guy, P. M. *Bioconjugate Chem.* **2009**, *20*, 404.
(9) Connally, R. E.; Piper, J. A. *Ann. N. Y. Acad. Sci.* **2008**, *1130*, 106.
(10) Bünzli, J.-C. G. *Chem. Lett.* **2009**, *38*, 104.
(11) Moore, E. G.; Samuel, A. P. S.; Raymond, K. N. *Acc. Chem. Res.* **2009**, *42*, 542.
(12) Dos Santos, C. M. G.; Harte, A. J.; Quinn, S. J.; Gunnlaugsson, T. *Coord. Chem. Rev.* **2008**, *252*, 2512.
(13) Hess, B. A.; Kedziorski, A.; Smentek, L.; Bornhop, D. J. *J. Phys. Chem. A* **2008**, *112*, 2397.
(14) Song, B.; Sivagnanam, V.; Vandevyver, C. D. B.; Hemmilä, I. A.; Lehr, H.-A.; Gijs, M. A. M.; Bünzli, J.-C. G. *Analyst* **2009**, *134*, 1991.
(15) Bünzli, J.-C. G.; Chauvin, A.-S.; Vandevyver, C. D. B.; Song, B.; Comby, S. *Ann. N. Y. Acad. Sci.* **2008**, *1130*, 97.
(16) Montgomery, C. P.; Murray, B. S.; New, E. J.; Pal, R.; Parker, D. *Acc. Chem. Res.* **2009**, *42*, 925.
(17) Fan, Y.; Yang, P.; Huang, S.; Jiang, J.; Lian, H.; Lin, J. *J. Phys. Chem. C* **2009**, *113*, 7628.
(18) Bünzli, J.-C. G.; Eliseeva, S. V. In *Springer Series on Fluorescence, Vol. 7, Lanthanide Spectroscopy, Materials, and Bio-applications*; Springer Verlag: Berlin, 2010; Chapter 2, in press.
(19) Nishioka, T., Fukui, K., Matsumoto, K. In *Handbook on the Physics and Chemistry of Rare Earths*; Gschneidner, K. A., Jr., Bünzli, J.-C. G., Pecharsky, V. K., Eds.; Elsevier Science BV: Amsterdam, 2007; Vol. 37, Chapter 234, p 171.
(20) Yuan, J.; Wang, G. *Trends Anal. Chem.* **2006**, *25*, 490.
(21) Eliseeva, S. V.; Ryazanov, M.; Gumy, F.; Troyanov, S. I.; Lepnev, L. S.; Bünzli, J.-C. G.; Kuzmina, N. P. *Eur. J. Inorg. Chem.* **2006**, 4809.
(22) Weissman, S. I. *J. Chem. Phys.* **1942**, *10*, 214.
(23) de Sá, G. F.; Malta, O. L.; Donega, C. D.; Simas, A. M.; Longo, R. L.; Santa-Cruz, P. A.; da Silva, E. F. *Coord. Chem. Rev.* **2000**, *196*, 165.

(24) Eliseeva, S. V.; Bünzli, J.-C. G. *Chem. Soc. Rev.* **2010**, *39*, 189.
(25) Blasse, G. *Struct. Bonding (Berlin)* **1976**, *26*, 45.
(26) Zolin, V. F.; Puntus, L. N.; Tsaryuk, V. I.; Kudryashova, V. A.; Legendziewicz, J.; Gawryszewska, P.; Szostak, R. *J. Alloys Compd.* **2004**, *380*, 279.
(27) Faulkner, S.; Natrajan, L. S.; Perry, W. S.; Sykes, D. *Dalton Trans.* **2009**, 3890.
(28) Imbert, D.; Cantuel, M.; Bünzli, J.-C. G.; Bernardinelli, G.; Piguet, C. *J. Am. Chem. Soc.* **2003**, *125*, 15698.
(29) Pope, S. J. A.; Coe, B. J.; Faulkner, S.; Bichenkova, E. V.; Yu, X.; Douglas, K. T. *J. Am. Chem. Soc.* **2004**, *126*, 9490.
(30) Lazarides, T.; Sykes, D.; Faulkner, S.; Barbieri, A.; Ward, M. D. *Chem.—Eur. J.* **2008**, *14*, 9389.
(31) Torelli, S.; Delahaye, S.; Hauser, A.; Bernardinelli, G.; Piguet, C. *Chem.—Eur. J.* **2004**, *10*, 3503.
(32) Lazarides, T.; Tart, N. M.; Sykes, D.; Faulkner, S.; Barbieri, A.; Ward, M. D. *Dalton Trans.* **2009**, 3971.
(33) Riis-Johannessen, T.; Dupont, N.; Canard, G.; Bernardinelli, G.; Hauser, A.; Piguet, C. *Dalton Trans.* **2008**, 3661.
(34) Lazarides, T.; Davies, G. M.; Adams, H.; Sabatini, C.; Barigelletti, F.; Barbieri, A.; Pope, S. J. A.; Faulkner, S.; Ward, M. D. *Photochem. Photobiol. Sci.* **2007**, *6*, 1152.
(35) Mehlstäubl, M.; Kottas, G. S.; Colella, S.; De Cola, L. *Dalton Trans.* **2008**, 2385.
(36) Xu, H. B.; Zhang, L. Y.; Chen, X. M.; Li, X. L.; Chen, Z. N. *Cryst. Growth Des.* **2009**, *9*, 569.
(37) Ziessel, R.; Diring, S.; Kadjane, P.; Charbonnière, L. J.; Retailleau, P.; Philouze, C. *Chem. Asian J.* **2007**, *2*, 975.
(38) Shavaleev, N. M.; Moorcraft, L. P.; Pope, S. J. A.; Bell, Z. R.; Faulkner, S.; Ward, M. D. *Chem. Commun.* **2003**, 1134.
(39) Comby, S. Bünzli, J.-C. G. In *Handbook on the Physics and Chemistry of Rare Earths*; Gschneidner, K. A., Jr., Bünzli, J.-C. G., Pecharsky, V. K., Eds.; Elsevier Science BV: Amsterdam, 2007; Vol. 37, Chapter 235, p 217.
(40) Bünzli, J.-C. G. *Acc. Chem. Res.* **2006**, *39*, 53.
(41) Görller-Walrand, C. Binnemans, K. In *Handbook on the Physics and Chemistry of Rare Earths*; Gschneidner, K. A., Jr., Eyring, L., Eds. Elsevier Science BV: Amsterdam, 1998; Vol. 25, Chapter 167, p 101.
(42) Shionoya, S.; Yen, W. M. *Phosphor Handbook*, 1st ed.; CRC Press Inc.: Boca Raton, FL, 1999.
(43) Carnall, W. T. In *Handbook on the Physics and Chemistry of Rare Earths*; Gschneidner, K. A., Jr., Eyring, L., Eds.; North Holland Publishing Co.: Amsterdam, 1979; Vol. 3, Chapter 24, p 172.
(44) Aebischer, A.; Gumy, F.; Bünzli, J.-C. G. *Phys. Chem. Chem. Phys.* **2009**, *11*, 1346.
(45) Shavaleev, N. M.; Scopelliti, R.; Gumy, F.; Bünzli, J.-C. G. *Inorg. Chem.* **2009**, *48*, 7937.
(46) Winkless, L.; Tan, R. H. C.; Zheng, Y.; Motevalli, M.; Wyatt, P. B.; Gillin, W. P. *Appl. Phys. Lett.* **2006**, 89 Art. 111115.
(47) Monguzzi, A.; Milani, A.; Lodi, L.; Trioni, M. I.; Tubino, R.; Castiglioni, C. *New J. Chem.* **2009**, *33*, 1542.
(48) Werts, M. H. V.; Jukes, R. T. F.; Verhoeven, J. W. *Phys. Chem. Chem. Phys.* **2002**, *4*, 1542.
(49) Ward, M. D. *Coord. Chem. Rev.* **2007**, *251*, 1663.
(50) Malta, O. L.; Brito, H. F.; Menezes, J. F. S.; Gonçalves e Silva, F. R.; Donega, C. D.; Alves, S. *Chem. Phys. Lett.* **1998**, *282*, 233.
(51) Bredol, M.; Kynast, U.; Ronda, C. *Adv. Mater.* **1991**, *3*, 361.
(52) Zucchi, G.; Maury, O.; Thuery, P.; Gumy, F.; Bünzli, J.-C. G.; Ephritikhine, M. *Chem.—Eur. J.* **2009**, *15*, 9686.
(53) Shavaleev, N. M.; Eliseeva, S. V.; Scopelliti, R.; Bünzli, J.-C. G. *Chem.—Eur. J.* **2009**, *15*, 10790.
(54) Filipescu, N.; Mushrush, G. W. *Nature* **1966**, *211*, 960.
(55) Kottas, G. S.; Mehlstaubl, M.; Froehlich, R.; De Cola, L. *Eur. J. Inorg. Chem.* **2007**, 3465.
(56) Brunet, E.; Juanes, O.; Sedano, R.; Rodriguez-Ubis, J.-C. *Photochem. Photobiol. Sci.* **2002**, *1*, 613.
(57) Fiedler, T.; Hilder, M.; Junk, P. C.; Kynast, U. H.; Lezhnina, M. M.; Warzala, M. *Eur. J. Inorg. Chem.* **2007**, 291.
(58) Biju, S.; Reddy, M. L. P.; Cowley, A. H.; Vasudevan, K. V. *J. Mater. Chem.* **2009**, *19*, 5179.
(59) Kajiwara, T.; Hasegawa, M.; Ishii, A.; Katagiri, K.; Baatar, M.; Takaishi, S.; Iki, N.; Yamashita, M. *Eur. J. Inorg. Chem.* **2008**, 5565.
(60) Petoud, S.; Cohen, S. M.; Bünzli, J.-C. G.; Raymond, K. N. *J. Am. Chem. Soc.* **2003**, *125*, 13324.
(61) Bünzli, J.-C. G. In *Lanthanide Probes in Life, Chemical and Earth Sciences. Theory and Practice*; Elsevier Science BV: Amsterdam, 1989; Chapter 7, pp 219.
(62) Beeby, A.; Clarkson, I. M.; Dickins, R. S.; Faulkner, S.; Parker, D.; Royle, L.; de Sousa, A. S.; Williams, J. A. G.; Woods, M. *J. Chem. Soc., Perkin Trans. 2* **1999**, 493.
(63) Kimura, T.; Kato, Y. *J. Alloys Compd.* **1998**, *271*, 867.
(64) Kimura, T.; Kato, Y. *J. Alloys Compd.* **1995**, *225*, 284.
(65) Horrocks, W. DeW., Jr.; Sudnick, D. R. *J. Am. Chem. Soc.* **1979**, *101*, 334.
(66) Supkowski, R. M.; Horrocks, W. DeW., Jr. *Inorg. Chim. Acta* **2002**, *340*, 44.
(67) Horrocks, W. DeW., Jr.; Sudnick, D. R. *Acc. Chem. Res.* **1981**, *14*, 384.
(68) Selvin, P. R. *Nat. Struct. Biol.* **2000**, *7*, 730.
(69) Torelli, S.; Imbert, D.; Cantuel, M.; Bernardinelli, G.; Delahaye, S.; Hauser, A.; Bünzli, J.-C. G.; Piguet, C. *Chem.—Eur. J.* **2005**, *11*, 3228.
(70) Charbonnière, L. J.; Hildebrandt, N.; Ziessel, R. F.; Lohmannsroben, H. G. *J. Am. Chem. Soc.* **2006**, *128*, 12800.
(71) Charbonnière, L. J.; Hildebrandt, N. *Eur. J. Inorg. Chem.* **2008**, 3241.
(72) Clapp, A. R.; Medintz, I. L.; Mattoussi, H. *ChemPhysChem* **2006**, *7*, 47.
(73) Stern, O.; Volmer, M. *Phys. Z.* **1919**, *20*, 183.
(74) Song, B.; Vandevyver, C. D. B.; Deiters, E.; Chauvin, A.-S.; Hemmilä, I. A.; Bünzli, J.-C. G. *Analyst* **2008**, *133*, 1749.
(75) Rodgers, S. J.; Lee, C. W.; Ng, C. Y.; Raymond, K. N. *Inorg. Chem.* **1987**, *26*, 1622.
(76) Diamandis, E. P. *Clin. Biochem.* **1988**, *21*, 139.
(77) Latva, M.; Takalo, H.; Mukkala, V. M.; Matachescu, C.; Rodriguez-Ubis, J.-C.; Kankare, J. *J. Lumin.* **1997**, *75*, 149.
(78) Mamedov, I.; Mishra, A.; Angelovski, G.; Mayer, H. A.; Palsson, L. O.; Parker, D.; Logothetis, N. K. *Dalton Trans.* **2007**, 5260.
(79) Hubbard, D. S.; Houlne, M. P.; Kiefer, G.; Bornhop, D. J. *SPIE Int. Soc. Opt. Eng.* **1997**, *2980*, 570.
(80) Comby, S.; Imbert, D.; Vandevyver, C. D. B.; Bünzli, J.-C. G. *Chem.—Eur. J.* **2007**, *13*, 936.
(81) Li, S. H.; Yuan, W. T.; Zhu, C. Q.; Xu, J. G. *Anal. Biochem.* **2004**, *331*, 235.
(82) Samuel, A. P. S.; Xu, J.; Raymond, K. N. *Inorg. Chem.* **2009**, *48*, 687.
(83) Yuan, J. L.; Matsumoto, K. *Anal. Sci.* **1996**, *12*, 695.
(84) Binnemans, K. In *Handbook on the Physics and Chemistry of Rare Earths*; Gschneidner, K. A., Jr., Bünzli, J.-C. G., Pecharsky, V. K., Eds.; Elsevier Science BV: Amsterdam, 2005; Vol. 35, Chapter 225, 107.
(85) Kleinerman, M. *J. Chem. Phys.* **1969**, *51*, 2370.
(86) Sato, S.; Wada, M. *Bull. Chem. Soc. Jpn.* **1970**, *43*, 1955.
(87) Archer, R. D.; Chen, H. Y.; Thompson, L. C. *Inorg. Chem.* **1998**, *37*, 2089.
(88) Green, N. M. *Biochem. J.* **1963**, *89*, 585.
(89) Prat, O.; Lopez, E.; Mathis, G. *Anal. Biochem.* **1991**, *195*, 283.
(90) Claudel-Gillet, S. P.; Steibel, J.; Weibel, N.; Chauvin, T.; Port, M.; Raynal, I.; Toth, E.; Ziessel, R. F.; Charbonnière, L. J. *Eur. J. Inorg. Chem.* **2008**, 2856.
(91) Zuchner, T.; Schumer, F.; Berger-Hoffmann, R.; Muller, K.; Lukas, M.; Zeckert, K.; Marx, J.; Hennig, H.; Hoffmann, R. *Anal. Chem.* **2009**, *81*, 9449.
(92) Yan, J.; Estevez, M. C.; Smith, J. E.; Wang, K.; He, X.; Wang, L.; Tan, W. *Nano Today* **2007**, *2*, 44.
(93) Ling, J. *SPIE Int. Soc. Opt. Eng.* **2008**, *6866*, Art. T8660.
(94) Hermanson, G. T. *Bioconjugate Techniques*, 2nd ed.; Academic Press, Elsevier: Amsterdam, 2008; Chapter 9.9, Lanthanide chelates for time-resolved fluorescence.
(95) Huhtinen, P.; Harma, H.; Lovgren, T. *Recent Res. Dev. Bioconjugate Chem.* **2005**, *2*, 85.
(96) Chatterjee, D. K.; Rufaihah, A. J.; Zhang, Y. *Biomaterials* **2008**, *29*, 937.
(97) Tsourkas, A.; Behlke, M. A.; Xu, Y. Q.; Bao, G. *Anal. Chem.* **2003**, *75*, 3697.
(98) Johansson, M. K.; Cook, R. M.; Xu, J. D.; Raymond, K. N. *J. Am. Chem. Soc.* **2004**, *126*, 16451.
(99) Bazin, H.; Guillemer, S.; Mathis, G. *J. Fluoresc.* **2002**, *12*, 245.
(100) Kitamura, Y.; Ihara, T.; Tsujimura, Y.; Osawa, Y.; Sasahara, D.; Yamamoto, M.; Okada, K.; Tazaki, M.; Jyo, A. *J. Inorg. Biochem.* **2008**, *102*, 1921.
(101) Escudier, J.-M.; Dupouy, C.; Fountain, M. A.; del Mundo, I. M. A.; Jacklin, E. M.; Morrow, J. R. *Org. Biomol. Chem.* **2009**, *7*, 3251.
(102) Martin, L. L.; Sculimbrene, B. R.; Nitz, M.; Imperiali, B. *QSAR Comb. Sci.* **2005**, *24*, 1149.
(103) Cisnetti, F.; Gateau, C.; Lebrun, C.; Delangle, P. *Chem.—Eur. J.* **2009**, *15*, 7456.
(104) Reynolds, A. M.; Sculimbrene, B. R.; Imperiali, B. *Bioconjugate Chem.* **2008**, *19*, 588.
(105) Parker, D. *Coord. Chem. Rev.* **2000**, *205*, 109.
(106) Gunnlaugsson, T.; Leonard, G. A. *Chem. Commun.* **2005**, 3114.
(107) Wolfbeis, O. S. *J. Mater. Chem.* **2005**, *15*, 2657.
(108) Borisov, S. M.; Wolfbeis, O. S. *Chem. Rev.* **2008**, *108*, 423.
(109) Prodi, L. *New J. Chem.* **2005**, *29*, 20.
(110) Hemmilä, I. *Applications of Fluorescence in Immunoassays*, 1st ed.; Wiley Interscience: New York, 1991.

(111) Xu, Y. Y.; Hemmilä, I.; Mukkala, V. M.; Holttinen, S.; Lövgren, T. *Analyst* **1991**, *116*, 1155.
(112) Mitrunen, K.; Pettersson, K.; Piironen, T.; Bjork, T.; Lilja, H.; Lovgren, T. *Clin. Chem.* **1995**, *41*, 1115.
(113) Evangelista, R. A.; Pollak, A.; Allore, B. D.; Templeton, A. F.; Morton, R. C.; Diamandis, E. P. *Clin. Biochem.* **1988**, *21*, 173.
(114) Oesterling, J. E.; Jacobsen, S. J.; Klee, G. G.; Pettersson, K.; Piironen, T.; Abrahamsson, P. A.; Stenman, U. H.; Dowell, B.; Lovgren, T.; Lilja, H. *J. Urol.* **1995**, *154*, 1090.
(115) Ye, Z. Q.; Tan, M. Q.; Wang, G. L.; Yuan, J. G. *Anal. Chem.* **2004**, *76*, 513.
(116) Harma, H.; Pelkkikangas, A. M.; Soukka, T.; Huhtinen, P.; Huopalahti, S.; Lovgren, T. *Anal. Chim. Acta* **2003**, *482*, 157.
(117) Jaras, K.; Tajudin, A. A.; Ressine, A.; Soukka, T.; Marko-Varga, G.; Bjartell, A.; Malm, J.; Laurell, T.; Lilja, H. *J. Proteome Res.* **2008**, *7*, 1308.
(118) Ollikka, P.; Ylikoski, A.; Kaatrasalo, A.; Harvala, H.; Hakala, H.; Hovinen, J. *Bioconjugate Chem.* **2008**, *19*, 1269.
(119) Morrison, L. E. *Anal. Biochem.* **1988**, *174*, 101.
(120) Morrison, L. E. Lifetime-resolved assay procedures. U.S. Patent 4,822,733, 1989.
(121) Guillaumont, D.; Bazin, H.; Benech, J. M.; Boyer, M.; Mathis, G. *ChemPhysChem* **2007**, *8*, 480.
(122) Petoud, S.; Bünzli, J.-C. G.; Glanzman, T.; Piguet, C.; Xiang, Q.; Thummel, R. P. *J. Lumin.* **1999**, *82*, 69.
(123) Gonçalves e Silva, F. R.; Longo, R. L.; Malta, O. L.; Piguet, C.; Bünzli, J.-C. G. *Phys. Chem. Chem. Phys.* **2000**, *2*, 5400.
(124) Trinquet, E.; Maurin, F.; Preaudat, M.; Mathis, G. *Anal. Biochem.* **2001**, *296*, 232.
(125) Maurel, D.; Kniazeff, J.; Mathis, G.; Trinquet, E.; Pin, J. P.; Ansanay, H. *Anal. Biochem.* **2004**, *329*, 253.
(126) Duthey, B.; Caudron, S.; Perroy, J.; Bettler, B.; Fagni, L.; Pin, J. P.; Prezeau, L. *J. Biol. Chem.* **2002**, *277*, 3236.
(127) Degorce, F.; Card, A.; Soh, S.; Trinquet, E.; Knapik, G. P.; Xie, B. *Curr. Chem. Genomics* **2009**, *3*, 22.
(128) Jin, D.; Connally, R.; Piper, J. *Cytometry, Part A* **2007**, *71A*, 783.
(129) Jin, D.; Connally, R.; Piper, J. *Cytometry, Part A* **2007**, *71A*, 797.
(130) Laitala, V.; Ylikoski, A.; Raussi, H. M.; Ollikka, P.; Hemmilä, I. *Anal. Biochem.* **2007**, *361*, 126.
(131) Mizukami, S.; Tonai, K.; Kaneko, M.; Kikuchi, K. *J. Am. Chem. Soc.* **2008**, *130*, 14376.
(132) Hagren, V.; von Lode, P.; Syrjala, A.; Soukka, T.; Lovgren, T.; Kojola, H.; Nurmi, J. *Anal. Biochem.* **2008**, *374*, 411.
(133) von Lode, P.; Rosenberg, J.; Pettersson, K.; Takalo, H. *Anal. Chem.* **2003**, *75*, 3193.
(134) Wang, M.; Mi, C.; Zhang, Y.; Liu, J.; Li, F.; Mao, C.; Xu, S. *J. Phys. Chem. C* **2009**, *113*, 19021.
(135) Soga, K. *Bunseki Kagaku* **2009**, *58*, 461.
(136) Wu, S. W.; Han, G.; Milliron, D. J.; Aloni, S.; Altoe, V.; Talapin, D. V.; Cohen, B. E.; Schuck, P. J. *Proc. Natl. Acad. Sci. U.S.A.* **2009**, *106*, 10917.
(137) Cooper, D. E.; D'Andrea, A.; Faris, G. W.; MacQueen, B.; Wright, W. H. In *Immunoassay and Other Bioanalytical Techniques*; CRC Press, Taylor & Francis Group: Boca Raton, FL, 2007; Chapter 9, p 217.
(138) Soukka, T.; Rantanen, T.; Kuningas, K. *Ann. N. Y. Acad. Sci.* **2008**, *1130*, 188.
(139) Spangler, C. M.; Spangler, C.; Schaerling, M. *Ann. N. Y. Acad. Sci.* **2008**, *1130*, 138.
(140) Yoshimura, E. Watanabe, T. In *Metal Ions in Biological Systems*; Sigel, A., Sigel, H., Eds. Marcel Dekker Inc.: New York, 2003; Vol. 40, Chapter 5, p 161.
(141) Yam, V. W. W.; Lo, K. K. W. *Coord. Chem. Rev.* **1999**, *184*, 157.
(142) Barrios, A. M.; Craik, C. S. *Bioorg. Med. Chem. Lett.* **2002**, *12*, 3619.
(143) Mitra, S.; Barrios, A. M. *Anal. Biochem.* **2007**, *370*, 249.
(144) Mitra, S.; Barrios, A. M. *ChemBioChem* **2008**, *9*, 1216.
(145) Terai, T.; Kikuchi, K.; Iwasawa, S.; Kawabe, T.; Hirata, Y.; Urano, Y.; Nagano, T. *J. Am. Chem. Soc.* **2006**, *128*, 6938.
(146) Tremblay, M. S.; Halim, M.; Sames, D. *J. Am. Chem. Soc.* **2007**, *129*, 7570.
(147) De Silva, A. P.; Gunaratne, H. Q. N.; Rice, T. E. *Angew. Chem., Int. Ed Engl.* **1996**, *35*, 2116.
(148) Gunnlaugsson, T.; Parker, D.; Williams, J. A. G. *SPIE Proc.* **1999**, *3602*, 186.
(149) Leonard, J. P.; Dos Santos, C. M. G.; Plush, S. E.; McCabe, D. J.; Gunnlaugsson, T. *Chem. Commun.* **2007**, 129.
(150) Parker, D.; Senanayake, P. K.; Williams, J. A. G. *J. Chem. Soc., Perkin Trans. 2* **1998**, 2129.
(151) McCoy, C. P.; Stomeo, F.; Plush, S. E.; Gunnlaugsson, T. *Chem. Mater.* **2006**, *18*, 4336.
(152) Bonnet, C. S.; Gunnlaugsson, T. *New J. Chem.* **2009**, *33*, 1025.
(153) Gunnlaugsson, T.; Mac Donaill, D. A.; Parker, D. *J. Am. Chem. Soc.* **2001**, *123*, 12866.
(154) Wang, Q. M.; Ogawa, K.; Toma, K.; Tamiaki, H. *J. Photochem. Photobiol., A* **2009**, *201*, 87.
(155) Sun, L.-N.; Peng, H.; Stich, M. I. J.; Achatz, D.; Wolfbeis, O. S. *Chem. Commun.* **2009**, 5000.
(156) Kauffman, D. R.; Shade, C. M.; Uh, H.; Petoud, S.; Star, A. *Nature Chem.* **2009**, *1*, 500.
(157) Borisov, S. M.; Wolfbeis, O. S. *Anal. Chem.* **2006**, *78*, 5094.
(158) Blair, S.; Kataky, R.; Parker, D. *New J. Chem.* **2002**, *26*, 530.
(159) Parker, D.; Williams, J. A. G. *Chem. Commun.* **1998**, 245.
(160) Ogawa, K.; Kobuke, Y. *Org. Biomol. Chem.* **2009**, *7*, 2241.
(161) Jiang, F. L.; Poon, C. T.; Wong, W. K.; Koon, H. K.; Mak, N. K.; Choi, C. Y.; Kwong, D. W. J.; Liu, Y. *ChemBioChem* **2008**, *9*, 1034.
(162) Zhou, J.; Liu, J.; Xia, S.; Wang, X.; Zhang, B. *J. Phys. Chem. B* **2005**, *109*, 19529.
(163) Hidek, E. *Cent. Eur. J. Biol.* **2008**, *3*, 273.
(164) Song, B.; Wang, G.; Tan, M.; Yuan, J. *J. Am. Chem. Soc.* **2006**, *128*, 13442.
(165) Song, B.; Wang, G.; Yuan, J. *Chem. Commun.* **2005**, 3553.
(166) Song, B.; Wang, G. L.; Tan, M. Q.; Yuan, J. L. *New J. Chem.* **2005**, *29*, 1431.
(167) Li, X.; Zhang, G.; Ma, H.; Zhang, D.; Li, J.; Zhu, D. *J. Am. Chem. Soc.* **2004**, *126*, 11543.
(168) Wolfbeis, O. S.; Durkop, A.; Wu, M.; Lin, Z. H. *Angew. Chem., Int. Ed.* **2002**, *41*, 4495.
(169) Jee, R. D. *Analyst* **1995**, *120*, 2867.
(170) Courrol, L. C.; Bellini, M. H.; Tarelho, L. V. G.; Silva, F. R. O.; Mansano, R. D.; Gomes, L.; Vieira, N. D.; Shor, N. *Anal. Biochem.* **2006**, *355*, 140.
(171) Courrol, L. C.; Samad, R. E. *Curr. Pharm. Anal.* **2008**, *4*, 238.
(172) Schaferling, M.; Wolfbeis, O. S. *Chem.—Eur. J.* **2007**, *13*, 4342.
(173) Hou, F. J.; Miao, Y. H.; Jiang, C. Q. *Spectrochim. Acta, Part A* **2005**, *61*, 2891.
(174) Hou, F. J.; Wang, X. L.; Jiang, C. Q. *Anal. Sci.* **2005**, *21*, 231.
(175) Shtykov, S. N.; Smirnova, T. D.; Bylinkin, Y. G. *J. Anal. Chem.* **2004**, *59*, 438.
(176) Duerkop, A.; Turel, M.; Lobnik, A.; Wolfbeis, O. S. *Anal. Chim. Acta* **2006**, *555*, 292.
(177) Schrenkhammer, P.; Rosnizeck, I. C.; Duerkop, A.; Wolfbeis, O. S.; Schaferling, M. *J. Biomol. Screening* **2008**, *13*, 9.
(178) Duerkop, A.; Aleksandrova, D.; Scripinets, Y.; Yegorova, A.; Vityukova, E. *Ann. N. Y. Acad. Sci.* **2008**, *1130*, 172.
(179) Charbonnière, L. J.; Mameri, S.; Kadjane, P.; Platas-Iglesias, C.; Ziessel, R. *Inorg. Chem.* **2008**, *47*, 3748.
(180) Spangler, C.; Spangler, C. M.; Spoerner, M.; Schaferling, M. *Anal. Bioanal. Chem.* **2009**, *394*, 989.
(181) Sambrook, J.; Russel, D. W. *Molecular Cloning: A Laboratory Manual*, 3rd ed.; Cold Spring Harbour Laboratory Press: New York, 2001.
(182) In *The Handbook: A Guide to Fluorescent Probes and Labelling Technologies*; Invitrogen: Carlsbad, CA, 2007; Chapter 8.1.
(183) Bonasera, V.; Alberti, S.; Sacchetti, A. *Biotechniques* **2007**, *43*, 173.
(184) Labarca, C.; Paigen, K. *Anal. Biochem.* **1980**, *102*, 344.
(185) Singer, V. L.; Jones, L. J.; Yue, S. T.; Haugland, R. P. *Anal. Biochem.* **1997**, *249*, 228.
(186) Vitzthum, F.; Geiger, G.; Bisswanger, H.; Brunner, H.; Bernhagen, J. *Anal. Biochem.* **1999**, *276*, 59.
(187) Schneeberger, C.; Speiser, P.; Kury, F.; Zeillinger, R. *PCR Methods Appl.* **1995**, *4*, 234.
(188) Leggate, J.; Allain, R.; Isaac, L.; Blais, B. W. *Biotechnol. Lett.* **2006**, *28*, 1587.
(189) Cesarone, C. F.; Bolognesi, C.; Santi, L. *Anal. Biochem.* **1979**, *100*, 188.
(190) Teare, J. M.; Islam, R.; Flanagan, R.; Gallagher, S.; Davies, M. G.; Grabau, C. *Biotechniques* **1997**, *22*, 1170.
(191) Glazer, A. N.; Rye, H. S. *Nature* **1992**, *359*, 859.
(192) Rye, H. S.; Yue, S.; Wemmer, D. E.; Quesada, M. A.; Haugland, R. P.; Mathies, R. A.; Glazer, A. N. *Nucleic Acids Res.* **1992**, *20*, 2803.
(193) Gudnason, H.; Dufva, M.; Bang, D. D.; Wolff, A. *Nucleic Acids Res.* **2007**, *35*, e127.
(194) Livak, K. J.; Flood, S. J. A.; Marmaro, J.; Giusti, W.; Deetz, K. *PCR Methods Appl.* **1995**, *4*, 357.
(195) Tyagi, S.; Kramer, F. R. *Nat. Biotechnol.* **1996**, *14*, 303.
(196) Whitcombe, D.; Theaker, J.; Guy, S. P.; Brown, T.; Little, S. *Nat. Biotechnol.* **1999**, *17*, 804.
(197) Ylikoski, A.; Elomaa, A.; Ollikka, P.; Hakala, H.; Mukkala, V. M.; Hovinen, J.; Hemmilä, I. *Clin. Chem.* **2004**, *50*, 1943.
(198) Nishioka, T., Yuan, J., Matsumoto, K. In *BioMEMS and Biomedical Nanotechnology* Springer Verlag: New York, 2006; Vol. 2, p 437.
(199) Laitala, V.; Hemmilä, I. *Anal. Chem.* **2005**, *77*, 1483.
(200) Bünzli, J.-C. G.; Piguet, C. *Chem. Soc. Rev.* **2005**, *34*, 1048.
(201) Chen, Y.; Lu, Z. H. *Anal. Chim. Acta* **2007**, *587*, 180.

(202) Chauvin, A.-S.; Comby, S.; Song, B.; Vandevyver, C. D. B.; Bünzli, J.-C. G. *Chem.—Eur. J.* **2008**, *14*, 1726.
(203) Hashino, K.; Ikawa, K.; Ito, M.; Hosoya, C.; Nishioka, T.; Makiuchi, M.; Matsumoto, K. *Anal. Biochem.* **2007**, *364*, 89.
(204) Nishioka, T.; Yuan, J.; Yamamoto, Y.; Sumitomo, K.; Wang, Z.; Hashino, K.; Hosoya, C.; Ikawa, K.; Wang, G.; Matsumoto, K. *Inorg. Chem.* **2006**, *45*, 4088.
(205) Kitamura, Y.; Ihara, T.; Tsujimura, Y.; Osawa, Y.; Tazaki, M.; Jyo, A. *Anal. Biochem.* **2006**, *359*, 259.
(206) Kitamura, Y.; Ihara, T.; Tsujimura, Y.; Osawa, Y.; Jyo, A. In Nucleic Acids Symposium Series; Oxford University Press: Oxford, 2006; Vol. 50, p 105.
(207) Escribano, P.; Julian-Lopez, B.; Planelles, A.; Cordoncillo, E.; Viana, B.; Sanchez, C. *J. Mater. Chem.* **2008**, *18*, 23.
(208) Son, A.; Dhirapong, A.; Dosev, D. K.; Kennedy, I. M.; Weiss, R. H.; Hristova, K. R. *Anal. Bioanal. Chem.* **2008**, *390*, 1829.
(209) Worlinsky, J. L.; Basu, S. *J. Phys. Chem. B* **2009**, *113*, 865.
(210) Nonat, A. M.; Quinn, S. J.; Gunnlaugsson, T. *Inorg. Chem.* **2009**, *48*, 4646.
(211) Bodi, A.; Borbas, K. E.; Bruce, J. I. *Dalton Trans.* **2007**, 4352.
(212) Pandya, S.; Yu, J. H.; Parker, D. *Dalton Trans.* **2006**, 2757.
(213) Parker, D. Williams, J. A. G. In *Metal Ions in Biological Systems*; Sigel, A., Sigel, H., Eds. Marcel Dekker Inc.: New York, 2003; Vol. 40, p 233.
(214) Thibon, A.; Pierre, V. C. *Anal. Bioanal. Chem.* **2009**, *394*, 107.
(215) Gunnlaugsson, T.; Ali, H. D. P.; Glynn, M.; Kruger, P. E.; Hussey, G. M.; Pfeffer, F. M.; Dos Santos, C. M. G.; Tierney, J. *J. Fluoresc.* **2005**, *15*, 287.
(216) Pal, R.; Parker, D. *Org. Biomol. Chem.* **2008**, *6*, 1020.
(217) Plush, S. E.; Gunnlaugsson, T. *Dalton Trans.* **2008**, 3801.
(218) Massue, J.; Quinn, S. J.; Gunnlaugsson, T. *J. Am. Chem. Soc.* **2008**, *130*, 6900.
(219) dos Santos, C. M. G.; Harte, A. J.; Quinn, S. J.; Gunnlaugsson, T. *Coord. Chem. Rev.* **2008**, *252*, 2512.
(220) Dos Santos, C. M. G.; Fernandez, P. B.; Plush, S. E.; Leonard, J. P.; Gunnlaugsson, T. *Chem. Commun.* **2007**, 3389.
(221) Ahrends, R.; Pieper, S.; Kuhn, A.; Weisshoff, H.; Hamester, M.; Lindemann, T.; Scheler, C.; Lehmann, K.; Taubner, K.; Linscheid, M. W. *Mol. Cell. Proteomics* **2007**, *6*, 1907.
(222) Pal, R.; Parker, D.; Costero, L. C. *Org. Biomol. Chem.* **2009**, *7*, 1525.
(223) Halim, M.; Tremblay, M. S.; Jockusch, S.; Turro, N. J.; Sames, D. *J. Am. Chem. Soc.* **2007**, *129*, 7704.
(224) Gunnlaugsson, T.; Stomeo, F. *Org. Biomol. Chem.* **2007**, *5*, 1999.
(225) Kataoka, Y.; Paul, D.; Miyake, H.; Yaita, T.; Miyoshi, E.; Mori, H.; Tsukamoto, S.; Tatewaki, H.; Shinoda, S.; Tsukube, H. *Chem.—Eur. J.* **2008**, *14*, 5258.
(226) Masaki, M. E.; Paul, D.; Nakamura, R.; Kataoka, Y.; Shinoda, S.; Tsukube, H. *Tetrahedron* **2009**, *65*, 2525.
(227) Tsukube, H.; Suzuki, Y.; Paul, D.; Kataoka, Y.; Shinoda, S. *Chem. Commun.* **2007**, 2533.
(228) Tsukube, H.; Yano, K.; Ishida, A.; Shinoda, S. *Chem. Lett.* **2007**, *36*, 554.
(229) Kataoka, Y.; Shinoda, S.; Tsukube, H. *J. Nanosci. Technol.* **2009**, *9*, 655.
(230) Sergent, N.; Levitt, J. A.; Green, M. A.; Suhling, K. *Proceedings SPIE* **2008**, 6861 Art. 68610K.
(231) Kankare, J.; Takalo, H.; Pasanen, P. Fluorescent lanthanide chelates. Patent EP 203047, 1986; 1990.
(232) Soini, E. J.; Pelliniemi, L. J.; Hemmilä, I. A.; Mukkala, V. M.; Kankare, J. J.; Frojdman, K. *J. Histochem. Cytochem.* **1988**, *36*, 1449.
(233) Gaiduck, M. I.; Grigoryants, V. V.; Mironov, A. F.; Rumyantseva, V. D.; Chissov, V. I.; Sukhin, G. M. *J. Photochem. Photobiol., B* **1990**, *7*, 15.
(234) Ke, H. Y. D.; Birnbaum, E. R.; Darnall, D. W.; Jackson, P. J.; Rayson, G. D. *Appl. Spectrosc.* **1992**, *46*, 479.
(235) Beverloo, H. B.; Van Schadewijk, A.; Van Gelderenboele, S.; Tanke, H. J. *Cytometry* **1990**, *11*, 784.
(236) Seveus, L.; Vaisala, M.; Syrjanen, S.; Sandberg, M.; Kuusisto, A.; Harju, R.; Salo, J.; Hemmilä, I.; Kojola, H.; Soini, E. *Cytometry* **1992**, *13*, 329.
(237) Seveus, L.; Vaisala, M.; Hemmilä, I.; Kojola, H.; Roomans, G. M.; Soini, E. *Microsc. Res. Tech.* **1994**, *28*, 149.
(238) Marriott, G.; Clegg, R. M.; Arndtjovin, D. J.; Jovin, T. M. *Biophys. J.* **1991**, *60*, 1374.
(239) Marriott, G.; Heidecker, M.; Diamandis, E. P.; Yanmarriott, Y. *Biophys. J.* **1994**, *67*, 957.
(240) Verwoerd, N. P.; Hennink, E. J.; Bonnet, J.; Vandergeest, C. R. G.; Tanke, H. J. *Cytometry* **1994**, *16*, 113.
(241) Phimphivong, S.; Kolchens, S.; Edmiston, P. L.; Saavedra, S. S. *Anal. Chim. Acta* **1995**, *307*, 403.
(242) Saavedra, S. S.; Picozza, E. G. *Analyst* **1989**, *114*, 835.
(243) Phimphivong, S.; Saavedra, S. S. *Bioconjugate Chem.* **1998**, *9*, 350.
(244) Vereb, G.; Jares-Erijman, E.; Selvin, P. R.; Jovin, T. M. *Biophys. J.* **1998**, *74*, 2210.
(245) de Haas, R. R.; Verwoerd, N. P.; van der Korput, M. P.; van Gijlswijk, R. P.; Siitari, H.; Tanke, H. J. *J. Histochem. Cytochem.* **1996**, *44*, 1091.
(246) Rulli, M.; Kuusisto, A.; Salo, J.; Kojola, H.; Simell, O. *J. Immunol. Methods* **1997**, *208*, 169.
(247) Vuorinen, P.; Rulli, M.; Kuusisto, A.; Simell, S.; Simell, T.; Vahlberg, T.; Ilonen, J.; Ty, H.; Knip, M.; Simell, O. *Ann. N. Y. Acad. Sci.* **2006**, *1079*, 226.
(248) Guo, W. H.; Ye, Z. Q.; Wang, G. L.; Zhao, X. M.; Yuan, J. L.; Du, Y. G. *Talanta* **2009**, *78*, 977.
(249) Calvo, W. J.; Lieber, B. B.; Hopkins, N.; Wakhloo, A. K. *Am. J. Neurorad.* **2001**, *22*, 691.
(250) Soini, A. E.; Kuusisto, A.; Meltola, N. J.; Soini, E.; Seveus, L. *Microsc. Res. Tech.* **2003**, *62*, 396.
(251) Rajapakse, H. E.; Reddy, D. R.; Mohandessi, S.; Butlin, N. G.; Miller, L. W. *Angew. Chem., Int. Ed.* **2009**, *48*, 4990.
(252) Connally, R.; Veal, D.; Piper, J. *FEMS Microbiol. Ecol.* **2002**, *41*, 239.
(253) Connally, R.; Jin, D. Y.; Piper, J. *Cytometry, Part A* **2006**, *69A*, 1020.
(254) Poole, R. A.; Montgomery, C. P.; New, E. J.; Congreve, A.; Parker, D.; Botta, M. *Org. Biomol. Chem.* **2007**, *5*, 2055.
(255) Yu, J. H.; Parker, D.; Pal, R.; Poole, R. A.; Cann, M. J. *J. Am. Chem. Soc.* **2006**, *128*, 2294.
(256) Frias, J. C.; Bobba, G.; Cann, M. J.; Hutchison, C. J.; Parker, D. *Org. Biomol. Chem.* **2003**, *1*, 905.
(257) Beeby, A.; Botchway, S. W.; Clarkson, I. M.; Faulkner, S.; Parker, A. W.; Parker, D.; Williams, J. A. G. *J. Photochem. Photobiol., B* **2000**, *57*, 83.
(258) Kielar, F.; Law, G. L.; New, E. J.; Parker, D. *Org. Biomol. Chem.* **2008**, *6*, 2256.
(259) New, E. J.; Parker, D. *Org. Biomol. Chem.* **2009**, *7*, 851.
(260) Hanaoka, K.; Kikuchi, K.; Kobayashi, S.; Nagano, T. *J. Am. Chem. Soc.* **2007**, *129*, 13502.
(261) Martin, L. J.; Hahnke, M. J.; Nitz, M.; Wohnert, J.; Silvaggi, N. R.; Allen, K. N.; Schwalbe, H.; Imperiali, B. *J. Am. Chem. Soc.* **2007**, *129*, 7106.
(262) Silvaggi, N. R.; Martin, L. J.; Schwalbe, H.; Imperiali, B.; Allen, K. N. *J. Am. Chem. Soc.* **2007**, *129*, 7114.
(263) Elhabiri, M.; Scopelliti, R.; Bünzli, J.-C. G.; Piguet, C. *J. Am. Chem. Soc.* **1999**, *121*, 10747.
(264) Bünzli, J.-C. G.; Comby, S.; Chauvin, A.-S.; Vandevyver, C. D. B. *J. Rare Earths* **2007**, *25*, 257.
(265) Vandevyver, C. D. B.; Chauvin, A.-S.; Comby, S.; Bünzli, J.-C. G. *Chem. Commun.* **2007**, 1716.
(266) Chauvin, A.-S.; Comby, S.; Song, B.; Vandevyver, C. D. B.; Bünzli, J.-C. G. *Chem.—Eur. J.* **2007**, *13*, 9515.
(267) Deiters, E.; Song, B.; Chauvin, A.-S.; Vandevyver, C. D. B.; Bünzli, J.-C. G. *New J. Chem.* **2008**, *32*, 1140.
(268) Deiters, E.; Song, B.; Chauvin, A.-S.; Vandevyver, C.; Bünzli, J.-C. G. *Chem.—Eur. J.* **2009**, *15*, 885.
(269) Song, B.; Vandevyver, C. D. B.; Chauvin, A.-S.; Bünzli, J.-C. G. *Org. Biomol. Chem.* **2008**, *6*, 4125.
(270) Dittrich, P. S.; Tachikawa, K.; Manz, A. *Anal. Chem.* **2006**, *78*, 3887.
(271) Laurell, T.; Petersson, F.; Nilsson, L. *Chem. Soc. Rev.* **2007**, *36*, 492.
(272) Ferrari, M. *Nature Rev. Cancer* **2005**, *5*, 161.
(273) Cheng, X.; Gupta, A.; Chen, C.; Tompkins, R. G.; Rodriguez, W.; Toner, M. *Lab Chip* **2009**, *9*, 1357.
(274) Fernandez-Moreira, V.; Song, B.; Sivagnanam, V.; Chauvin, A.-S.; Vandevyver, C. D. B.; Gijs, M. A. M.; Hemmilä, I. A.; Lehr, H.-A.; Bünzli, J.-C. G. *Analyst* **2010**, *135*, 42.
(275) Xu, C.; Zipfel, W.; Shear, J. B.; Williams, R. M.; Webb, W. W. *Proc. Natl. Acad. Sci. U.S.A.* **1996**, *93*, 10763.
(276) Hanninen, P.; Soukka, J.; Soini, J. T. *Ann. N. Y. Acad. Sci.* **2008**, *1130*, 320.
(277) Kielar, F.; Congreve, A.; Law, G. L.; New, E. J.; Parker, D.; Wong, K. L.; Castreno, P.; de Mendoza, J. *Chem. Commun.* **2008**, 2435.
(278) Palsson, L. O.; Pal, R.; Murray, B. S.; Parker, D.; Beeby, A. *Dalton Trans.* **2007**, 5726.
(279) Eliseeva, S., Auböck, G., van Mourik, F., Cannizo, A., Song, B., Deiters, E., Chauvin, A.-S., Chergui, M., Bünzli, J.-C. G. *J. Phys. Chem. B* **2010**, in press, DOI 10.1021/jp9090206.
(280) He, G. S.; Tan, L. S.; Zheng, Q.; Prasad, P. N. *Chem. Rev.* **2008**, *108*, 1245.
(281) Andraud, C.; Maury, O. *Eur. J. Inorg. Chem.* **2009**, *29—30*, 4357.
(282) Picot, A.; D'Aléo, A.; Baldeck, P. L.; Grichine, A.; Duperray, A.; Andraud, C.; Maury, O. *J. Am. Chem. Soc.* **2008**, *130*, 1532.
(283) D'Aléo, A.; Picot, A.; Baldeck, P. L.; Andraud, C.; Maury, O. *Inorg. Chem.* **2008**, *47*, 10269.
(284) Picot, A.; Malvolti, F.; LeGuennic, B.; Baldeck, P. L.; Williams, J. A. G.; Andraud, C.; Maury, O. *Inorg. Chem.* **2007**, *46*, 2659.

(285) McRae, R.; Bagchi, P.; Sumalekshmy, S.; Fahrni, C. J. *Chem. Rev.* **2009**, *109*, 4780.
(286) Kim, H. M.; Cho, B. R. *Acc. Chem. Res.* **2009**, *42*, 863.
(287) Yu, M. X.; Li, F. Y.; Chen, Z. G.; Hu, H.; Zhan, C.; Yang, H.; Huang, C. H. *Anal. Chem.* **2009**, *81*, 930.
(288) Lim, S. F.; Riehn, R.; Ryu, W. S.; Khanarian, N.; Tung, C. K.; Tank, D.; Austin, R. H. *Nano Lett.* **2006**, *6*, 169.
(289) Yu, X. F.; Chen, L. D.; Li, M.; Xie, M. Y.; Zhou, L.; Li, Y.; Wang, Q. Q. *Adv. Mater.* **2008**, *20*, 4118.
(290) Wong, K. L.; Law, G. L.; Murphy, M. B.; Tanner, P. A.; Wong, W. T.; Lam, P. K.-S.; Lam, M. H.-W. *Inorg. Chem.* **2008**, *47*, 5190.
(291) Makhluf, S. B.-D.; Arnon, R.; Patra, C. R.; Mukhopadhyay, D.; Gedanken, A.; Mukherjee, P.; Breitbart, H. *J. Phys. Chem. C* **2008**, *112*, 12801.
(292) Li, L.; Liu, Y.; Tao, J.; Zhang, M.; Pan, H.; Xu, X.; Tang, R. *J. Phys. Chem. C* **2008**, *112*, 12219.
(293) Wu, J.; Ye, Z.; Wang, G.; Jin, D.; Yuan, J.; Guang, Y.; Piper, J. *J. Mater. Chem.* **2009**, *19*, 1258.
(294) Amiot, C. L.; Xu, S. P.; Liang, S.; Pan, L. Y.; Zhao, J. X. J. *Sensors* **2008**, *8*, 3082.
(295) Petoud, S. Polymetallic luminescent lanthanide dendrimer complexes for biological imaging in cells and small animals. Annual meeting, COST Action D38, Warsaw, April 25−27, 2009, abstract O1.
(296) Nagl, S.; Stich, M. I. J.; Schaferling, M.; Wolfbeis, O. S. *Anal. Bioanal. Chem.* **2009**, *393*, 1199.
(297) Sivagnanam, V.; Song, B.; Vandevyver, C. D. B.; Gijs, M. A. M. *Anal. Chem.* **2009**, *81*, 6509.
(298) Moriggi, L.; Aebischer, A.; Cannizzo, C.; Sour, A.; Borel, A.; Bünzli, J.-C. G.; Helm, L. *Dalton Trans.* **2009**, 2088.
(299) Pellegatti, L.; Zhang, J.; Drahos, B.; Villette, S.; Suzenet, F.; Guillaumet, G.; Petoud, S.; Toth, E. *Chem. Commun.* **2008**, 6591.
(300) Koullourou, T.; Natrajan, L. S.; Bhavsar, H.; Pope, S. J. A.; Feng, J. H.; Narvainen, J.; Shaw, R.; Scales, E.; Kauppinen, R.; Kenwright, A. M.; Faulkner, S. *J. Am. Chem. Soc.* **2008**, *130*, 2178.
(301) Jin, T.; Yoshioka, Y.; Fujii, F.; Komai, Y.; Seki, J.; Seiyama, A. *Chem. Commun.* **2008**, 5764.
(302) Rieter, W. J.; Kim, J. S.; Taylor, K. M. L.; An, H. Y.; Lin, W.; Tarrant, T.; Lin, W. B. *Angew. Chem., Int. Ed.* **2007**, *46*, 3680.
(303) Picard, C.; Geum, N.; Nasso, I.; Mestre, B.; Tisnes, P.; Laurent, S.; Muller, R. N.; Vander Elst, L. *Bioorg. Med. Chem. Lett.* **2006**, *16*, 5309.
(304) Bryson, J. M.; Fichter, K. M.; Chu, W. Y.; Lee, H. J.; Li, J.; Madsen, L. A.; McLendon, P. M.; Reineke, T. M. *Proc. Natl. Acad. Sci. U.S.A.* **2009**, *106*, 16913.

CR900362E